Half-lives for Highly Forbidden Unique Beta Decays in Medium-heavy Nuclei

Joel Kostensalo*
University of Jyväskylä, Department of Physics,
Post Office Box 35 (YFL), FI-40014, Finland

(Dated: November 4, 2016)

Half-lives for 2^{nd}, 3^{rd}, 4^{th}, 6^{th} and 7^{th} forbidden unique beta transitions were calculated using nuclear matrix elements (NME) given by both proton-neutron quasiparticle random phase approximation (pnQRPA) and two-quasiparticle NMEs. The decays fell into two groups: in the first one, mostly consisting of non-magic nuclei, the ratio of pnQRPA and two-particle matrix elements was 0.41 ± 0.12. In the other group consisting of mainly higher forbidden semi-magic nuclei the ratio of the NMEs was much smaller, about 0.004. The NMEs of semi-magic nuclei were found to heavily depend on the single-particle energies used in the pnQRPA calculation, while non-magic were not. This was inferred to be caused by the sharp Fermi-surface given by BCS for the non-magic nuclei. Since overall the behavior of the NMEs was similar to the earlier study with these models, it was suggested that the ratio of observed half-lives to the ones produced by pnQRPA most likely behave in the same way as in the case of Gamow-Teller decays. The still unmeasured half-lives for these transitions were predicted to be around 1.5-4.7 times longer than the ones given by pnQRPA depending on the mass number A.

I. INTRODUCTION

The single β-decay process has been well understood for decades (see e.g. [1]), and has been backed up by countless experiments. For quite a while the research of single β-decay has been focused on the ultra-low Q-value and forbidden cases [2–9]. However, predicting nuclear observables is not straightforward, and any given nuclear model tends to produce good results only for some region of the nuclear landscape. Recent research regarding the spin-dipole (SD) and Gamow-Teller nuclear matrix elements (NMEs) has shown that the observed NMEs of medium-heavy nuclei are reduced by a constant factor compared to the ones predicted by two-quasiparticle (two-qp) and proton-neutron random-phase approximation (pnQRPA) [10, 11]. These reductions were inferred to be caused by the spin-isospin correlations, and the nuclear medium effects not explicitly included in the pnQRPA model. A similar study regarding the magnetic hexadecapole NMEs showed that the observed NME is reduced by a constant factor with respect to the two-qp and the microscopic qp-phonon model (MQPM) NMEs [12].

In the present article we look at the half-lives of second and higher forbidden unique β-decays given by the two-qp and pnQRPA models. In a K^{th} forbidden unique beta decay the difference in the angular momenta of the mother and daughter nuclei is $\Delta J = K + 1$, and the parity changes in the odd-forbidden and remains the same in even-forbidden decays [13]. The change in angular momentum and parity for different degrees of forbiddeness is presented in table I. Based on the half-lives predicted by two-qp and pnQRPA models, we make a prediction of the factor by which the observed half-lives are increased with respect to the pnQRPA half-lives. These predictions can be used to optimally design an experiment for the measurement of the half-lives.

The nuclear β-decay research has been recently focused on the neutrino-less double-β-decay and astro-neutrino-nuclear processes. These aim to gain knowledge of the Majorana properties and absolute mass-scales of neutrinos [14–19]. The neutrino-less double-β-decay has not yet been experimentally observed. The half-lives for double-β-decays are extremely long, and competing processes can make the detection of a double-β-decay very hard. The knowledge of the half-lives of highly forbidden decays competing with the decay of interest is necessary. For example the experimentally observed $2\nu\beta^-$-decay of ^{48}Ca has competing non-unique and unique single-β-decay modes to the 4^+, 5^+ and 6^+ states in ^{48}Ca [4, 5].

The theoretical prediction of single and double-β-decay half-lives is not without issues. The value of the axial vector coupling constant g_A and the particle-particle interaction parameter g_{pp} of pnQRPA have not been given a clear value [20]. The g_{pp} values of approximately $0.6-0.8$ and quenched g_A values of approximately $0.6-0.7$ seem to make the pnQRPA and experimental doubleβ-decay NMEs agree [21, 22]. The issues with g_{pp} effecting the determination of g_A are discussed in [23]. The decay rates depend on the second power of g_A for the single and on the fourth power for double-β-decays, and so the understanding of the behavior of g_A is important for more accurate predictions of half-lives. In the articles [20] and [11] g_A was studied using the NMEs of forbidden non-unique and GT transitions. The studies suggest that g_A is a function of mass number A instead of being constant as assumed in the calculations of the present paper. The data from unique forbidden decays might also be used in this way for the determination of the g_A in the future.

* joel.j.kostensalo@student.jyu.fi

TABLE I. The change in angular momentum and parity in a K^{th} forbidden unique decay.

K	1	2	3	4	5	6
ΔJ	2	3	4	5	6	7
$\pi_i\pi_f$	-1	+1	-1	+1	-1	+1

II. THEORETICAL FORMALISM

In this section we give a short overview of the theory behind the calculations performed. The theoretical half-lives of K^{th} forbidden unique β-decays are defined in terms of reduced transition probabilities B_{Ku} and phase-space factors f_{Ku}. The B_{Ku} is given by the nuclear matrix element (NME), which in turn is given by the two-qp NMEs and one-body transition densities. The half-life can be written as [13]

$$t_{1/2} = \frac{\kappa}{f_{Ku}B_{Ku}}, \tag{1}$$

where κ is a constant with value [24]

$$\kappa = \frac{2\pi^3\hbar^7 \ln 2}{m_e^5 c^4 G_F^2} = 6147 \text{ s}. \tag{2}$$

A. Phase-Space Factor

The phase-space factor $f_{Ku}^{(\pm)}$ for the K^{th} forbidden unique $\beta^{\pm}$-decay is [13]

$$f_{Ku}^{\mp} = \left(\frac{3}{4}\right)^K \frac{(2K)!!}{(2K+1)!!}\int_1^{E_0} S_{Ku}^{(\mp)}(Z_f,\epsilon)\mathrm{d}\epsilon, \tag{3}$$

where $S_{KU}^{(\mp)}$ is the shape function, which depends on the degree of forbiddeness. The shape function can be approximated for example using the *Primakoff-Rosen*-approximation presented in the reference [25], but in order to get a more realistic values for the phase-space factor, the exact expressions presented in [26] were used in this work. The phase-space factor used for the *EC*-decays is presented in [27]. The general formulation for calculating phase-space factors is presented rigorously in [1]. The non-unique case is also presented in great detail in [3].

B. Reduced Beta Transition Probability

The reduced beta transition probability can be written in terms of the NME M_{Ku} as

$$B_{Ku} = \frac{g_A^2}{2J_i+1}|M_{Ku}|^2, \tag{4}$$

where J_i is the angular momentum of the mother nucleus, and g_A is the axial-vector coupling constant for which the value $g_A = 1.25$ was used. However, it should be noticed that the value of g_A is affected by many-nucleon correlations, and a value reduced by 20–30% is used in some sources [13]. The NME can be expressed as [13]

$$M_{Ku} = \sum_{ab} M^{(Ku)}(ab)(\psi_f||[c_a^\dagger \tilde{c}_b]_{K+1}||\psi_i), \tag{5}$$

where the factors $M^{(Ku)}$ are the two-qp matrix elements and the quantities $(\psi_f||[c_a^\dagger\tilde{c}_b]_{K+1}||\psi_i)$ are the one-body transition densities with ψ_i being the initial and ψ_f being the final nuclear wave functions. The two-qp matrix elements are given by [13]

$$M^{(Ku)}(ab) = (2,590\cdot 10^{-3}\cdot b\ [fm])^K m^{(Ku)}(ab), \tag{6}$$

where b is the oscillator length given by

$$b = \frac{197,33}{\sqrt{940\cdot(45A^{1/3}-25A^{-2/3})}}\text{ fm}. \tag{7}$$

In the equation (6) the quantity $m^{(Ku)}$ is the scaled two-qp matrix element given in the CS sign convention as

$$\begin{aligned} m^{(Ku)} =& \frac{1}{2\sqrt{(K+1)(2K+3)}}(-1)^{l_a+j_a+j_b+K+1} \\ &\times \frac{1+(-1)^{l_a+l_b+K}}{2}\hat{j_a}\hat{j_b}\begin{pmatrix} j_a & j_b & K+1 \\ \frac{1}{2} & \frac{-1}{2} & 0\end{pmatrix} \\ &\times [(-1)^K \hat{j_a}^2 + (-1)^{j_a+j_b+1}\hat{j_b}^2 \\ &+ 2(K+1)(-1)^{l_a+j_a+K-\frac{1}{2}}]\tilde{R}_{ab}^{(K)}, \end{aligned} \tag{8}$$

where the j_i and l_i stand for the angular momentum and orbital angular momentum of the orbital i respectively and $\tilde{R}_{ab}^{(K)}$ is the scaled radial integral. The calculation of the radial integral is discussed in detail in for example [13].

The one-body transition densities in (5) can be written in the pnQRPA picture for β^--decay as [28]

$$(\omega_f||[c_p^\dagger\tilde{c}_n]_K||0_{g.s.}^+) = \delta_{KJ_f}\hat{J}_f(u_pv_nX_{pn}^{\omega_f} + v_pu_nY^{\omega_f}pn), \tag{9}$$

where the pnQRPA vacuum 0^+ is the ground state of the even-even nucleus in the transition, and u and v are the unoccupation and occupation amplitudes given by BCS-theory. For the β^+/EC-decays the unoccupation and occupation amplitudes need to be exchanged ($u \leftrightarrow v$). The two-qp matrix element can be calculated by setting $X = 1$ and $Y = 0$. The unoccupation and occupation amplitudes can be calculated from the BCS equations (see formulation [13]). The final state ω_f is [29]

$$|\omega_f\rangle = \sum_{pn}(X_{pn}^{\omega_f}[a_p^\dagger a_n^\dagger]_{J_f} + Y_{pn}^{\omega_f}[\tilde{a}_p\tilde{a}_n]_{J_f})|\text{pnQRPA}\rangle, \tag{10}$$

where X and Y are the forward and backward going amplitudes, $a^\dagger$ and $\tilde{a}$ are the BCS quasiparticle creation and annihilation operators and $|\text{pnQRPA}\rangle$ is the pnQRPA vacuum.

III. NUMERICAL APPLICATION OF THE FORMALISM

Half-lives and partial half-lives were calculated for sixty β^- and β^+/EC transitions. This was done with both the two-qp model and the more advanced pnQRPA approach. In the two-qp model the transition is presumed to happen between the two single-particle states which gave the largest absolute value for the NME, while in the pnQRPA all possible configurations producing the initial and final states were taken into consideration.
The single-particle energies needed to solve the BCS equations were calculated using the Woods-Saxon potential. For nuclei with mass number A=50–60 the core was chosen to consist of eight protons and neutrons with the valence space 0d5/2 − 0g9/2. For the nuclei with larger A a core of 20 protons and neutrons was assumed. For A=74 the valence space was chosen as 0f7/2 − 0h11/2, for A=86-108 as 0f7/2 − 0h9/2, and for A=110–146 as 0f7/2 − 2p1/2. For the calculations of half-lives a value of 1.0 was used for the particle-particle and particle-hole interaction matrix elements. The uncertainty of the half-life due to the error in the NME was approximated by letting these parameters vary by 10% from the default value of 1.

The Q-values and their uncertainties found in [30] were used for the calculation of the phase-space factors and their contribution to the uncertainties of the half-lives. In the calculation of the shape functions given in [26] were used.

IV. RESULTS AND DISCUSSION

The calculated half-lives and their uncertainties are listed in the tables II-VI for each degree of forbiddeness separately. The half-lives vary by many orders of magnitude since the proton number, decay mode $\beta^{\pm}$, reduction or increase of the Q-value of about 1 MeV, and whether the decay is to or from the pnQRPA vacuum all increase/decrease the half-life by approximately one order of magnitude, and one degree of forbiddeness changes the half-life by close to four orders of magnitude. The differences in the Q-values from around 100 keV to the enormous 9.3 MeV of the second forbidden decay ^{52}Sc(3+) → ^{52}Ti(0+) alone is enough to make a difference of up to nine magnitudes.

Many of the studied decays are a part of a long decay chain including decays with different degrees of forbiddeness. In figure 1 the simple decay chain of the studied $A = 110$ nuclei is presented. The chain consists purely of ground-state-to-ground-state β^+/EC-decays. In figure 2 the more complicated $A = 96$ chain is presented. This chain includes both β^+/EC and β^--decays, and some of the decays are to and from excited states.

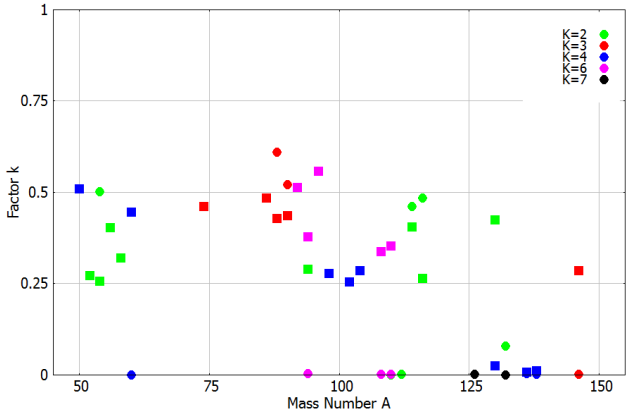

FIG. 3. The ratio $k = M^m_{\rm pnQRPA}/M^m_{\rm qp}$ as a function of mass number A. The degree of forbiddeness K is marked by color. The semi-magic and doubly magic nuclei are represented by circles and the non-magic nuclei by squares. For mass numbers with several non-magic nuclei the geometric mean was used.

In order to determine how the experimental values of the half-lives of these decays will most likely differ from the values given by the models, we'll compare our results to the first forbidden case and the results gotten from studying Gamow-Teller decays. In the letter [10] the authors looked at the values of experimental, pnQRPA and two-qp spin-dipole (SD) NMEs. They found that the ratio $M^m_{\rm QRPA}/M^m_{\rm qp}$ was approximately 0.4, while the ratio $M^m_{\rm exp}/M^m_{\rm QRPA}$ was about 0.5, where the M^ms stand for the geometric mean of β^+ and β^- NMEs with a common mother or daughter nucleus. Using all nuclei with the same A instead of just those with a common mother or daughter nuclei did not seem to effect the behavior as seen in figures 3 and 4. Therefore all nuclei with the same A was used to get more data. In a study regarding the mean matrix elements of Gamow-Teller (GT) decays the ratio $M^m_{\rm QRPA}/M^m_{\rm qp}$ was found to be approximately 0.38, and the ratio $M^m_{\rm exp}/M^m_{\rm QRPA}$ was found to be about 0.6 [11]. This study included a large number of decays, and the behavior of k as a function of A was determined in much more detail than in the earlier study regarding SD NMEs. For the second or higher forbidden decays we don't have experimental data, but we can still calculate the ratio of the geometric means of pnQRPA and two-qp NMEs. By comparing this ratio to the ones of SD and GT matrix elements, we can make a prediction of the ratio $M^m_{\rm exp}/M^m_{\rm QRPA}$ in which we are interested in.

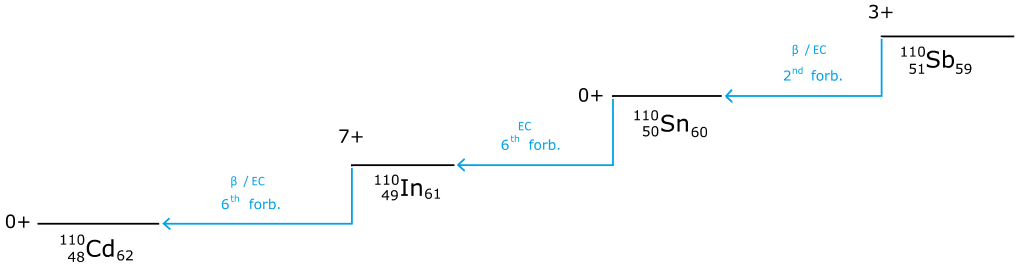

FIG. 1. The decay chain of the studied $A = 110$ nuclei.

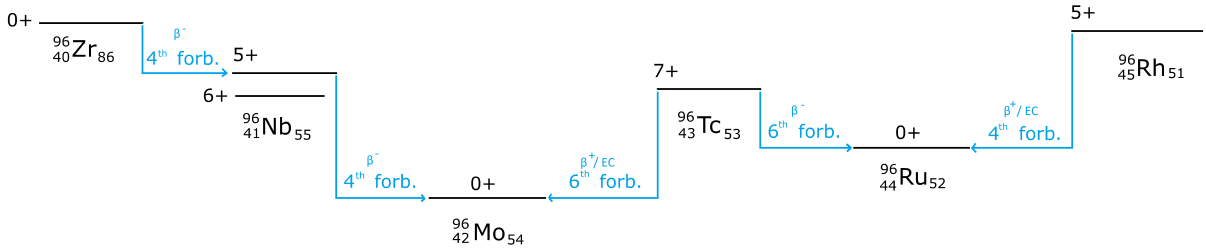

FIG. 2. The decay chain of the studied $A = 96$ nuclei.

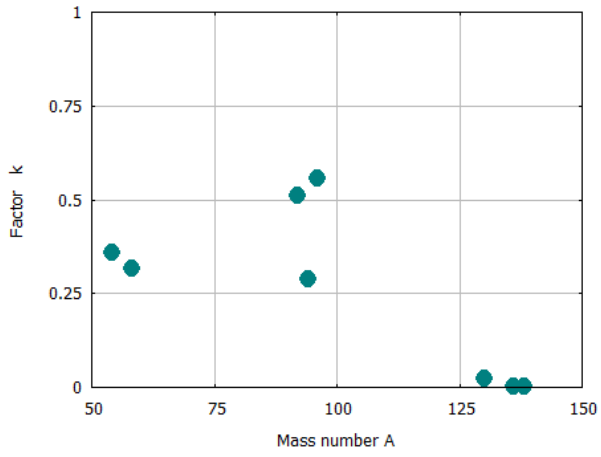

FIG. 4. Geometric mean of the ratio $k = M_{\rm pnQRPA}/M_{\rm qp}$ of the $\beta^{\pm}$ decay NMEs with a common mother or daughter nucleus.

In the tables II-VI it seems that for most decays the half-lives given by pnQRPA are about 5-10 times longer than those given by two-qp model regardless of the degree of forbiddeness. However, there seems to be some noticeable exceptions. The pnQRPA half-lives seem to be around 4-5 magnitudes longer for most of the decays including a semi-magic nucleus than the ones given by the two-qp model. For the only doubly magic nucleus ^{132}Sn this ratio seemed to also be large. Since the ratios of the NMEs are so wildly different, it is best to to study it separately for semi-magic and non-magic nuclei. In figure 3 the geometric means of the ratios $M_{\rm QRPA}/M_{\rm qp}$ for non-magic nuclei with the same mass number A are plotted as function of A along with the unmodified ratios of semi-magic NMEs for different degrees of forbiddeness. From the figure 3 one can see that there are clearly two distinct groups: in one group k is mostly around 0.25-0.6 and in the other k is 0.01 or less. Most NMEs fall into the first group, and only one fifth are in the second group. Only couple of the decays the ratio of NMEs was between 0.01 and 0.25. Taking the average of the first group (those with $k > 0.01$) and the standard deviation as the uncertainty one finds that the reduction factor k for them is

$$k = \frac{M^m_{pnQRPA}}{M^m_{qp}} = 0.41 \pm 0.12. \qquad (11)$$

In figure 3 the NMEs seem to fall into thee regions, for which A=50-88, A=89-121 and A=122-146. In the first two regions k seems to be roughly the same, but in the

TABLE II. Computed (partial) half-lives for second forbidden unique β^-, β^+ and EC decays with pnQRPA and two-qp models and the used NMEs. The transitions are (0+) $\leftrightarrow$ (3+), where (0+) is the ground state in the even-even-nucleus of the decay. The expected experimental half-lives are scaled from the pnQRPA half-lives with the scaling factor ξ presented in table VIII.

Transition	Mode	Two-qp	$\lvert M_{\mathrm{pnQRPA}}\rvert$	$\lvert M_{\mathrm{qp}}\rvert$	$t_{1/2(\mathrm{QRPA})}$	$t_{1/2(\mathrm{QP})}$	Expected $t_{1/2}$
^{52}Ti $\rightarrow$ ^{52}V	β^-	$0d_{3/2} - 0g_{9/2}$	$1.82 \cdot 10^{-4}$	$6.68 \cdot 10^{-4}$	57(2) a	4.3(2) a	125(5) a
^{52}Sc $\rightarrow$ ^{52}Ti	β^-	$0d_{3/2} - 0g_{9/2}$	$1.82 \cdot 10^{-4}$	$6.68 \cdot 10^{-4}$	9.9(2) h	52(1) min	21.8(5) h
^{54}Mn $\rightarrow$ ^{54}Fe	β^-	$0d_{3/2} - 0g_{9/2}$	$3.43 \cdot 10^{-4}$	$6.83 \cdot 10^{-4}$	$1.9(3) \cdot 10^5$ a	$4.8(6) \cdot 10^4$ a	$9.2(7) \cdot 10^5$ a
^{54}Mn $\rightarrow$ ^{54}Cr	EC	$0g_{9/2} - 0d_{3/2}$	$1.77 \cdot 10^{-4}$	$6.88 \cdot 10^{-4}$	$3.2(7) \cdot 10^5$ a	$2.1(4) \cdot 10^4$ a	$7(2) \cdot 10^5$ a
	β^+				$3.8(7) \cdot 10^8$ a	$2.5(5) \cdot 10^7$ a	$9(2) \cdot 10^8$ a
	EC/β^+				$3.2(7) \cdot 10^5$ a	$2.1(4) \cdot 10^4$ a	$7(2) \cdot 10^5$ a
^{56}Cr $\rightarrow$ ^{56}Mn	β^-	$0d_{3/2} - 0g_{9/2}$	$2.80 \cdot 10^{-4}$	$6.78 \cdot 10^{-4}$	97.6(9) a	35(4) a	210(2) a
^{56}Mn $\rightarrow$ ^{56}Fe	β^-	$0d_{3/2} - 0g_{9/2}$	$2.72 \cdot 10^{-4}$	$6.87 \cdot 10^{-4}$	1.17(6) a	67(4) d	2.6(2) a
^{58}Mn $\rightarrow$ ^{58}Fe	β^-	$0d_{3/2} - 0g_{9/2}$	$2.98 \cdot 10^{-4}$	$6.89 \cdot 10^{-4}$	3.39(5) d	15.2(2) h	7.5(1) d
^{58}Co $\rightarrow$ ^{58}Fe	EC	$0g_{9/2} - 0d_{3/2}$	$1.66 \cdot 10^{-4}$	$7.02 \cdot 10^{-4}$	$9.5(3) \cdot 10^3$ a	530(20) a	$2.09(7) \cdot 10^4$ a
	β^+				2.5(2) a	$1.38(9) \cdot 10^3$ a	5.5(5) a
	EC/β^+				6.9(3) a	380(20) a	15.2(7) a
^{94}Nb $\rightarrow$ ^{94}Mo	β^-	$0f_{5/2} - 0h_{11/2}$	$2.96 \cdot 10^{-4}$	$1.13 \cdot 10^{-3}$	54(4) a	3.7(3) a	119(9) a
^{94}Nb $\rightarrow$ ^{94}Zr	β^+	$0h_{11/2} - 0f_{5/2}$	$3.78 \cdot 10^{-4}$	$1.18 \cdot 10^{-3}$	$1.4(3) \cdot 10^5$ a	$1.4(3) \cdot 10^4$ a	$3.1(6) \cdot 10^5$ a
^{110}Sb $\rightarrow$ ^{110}Sn	EC	$0h_{11/2} - 0f_{5/2}$	$2.93 \cdot 10^{-7}$	$1.23 \cdot 10^{-3}$	$1.8(2) \cdot 10^5$ a	3.6(3) d	$4.5(8) \cdot 10^5$ a
	β^+				$1.7(2) \cdot 10^4$ a	8.3(7) h	$8.5(6) \cdot 10^4$ a
	EC/β^+				$1.5(2) \cdot 10^4$ a	7.6(6) h	$7.0(8) \cdot 10^4$ a
^{112}Sb $\rightarrow$ ^{112}Sn	EC	$0h_{11/2} - 0f_{5/2}$	$1.53 \cdot 10^{-6}$	$1.24 \cdot 10^{-3}$	$1.8(2) \cdot 10^4$ a	10.2(8) d	$8.5(8) \cdot 10^4$ a
	β^+				$3.3(3) \cdot 10^3$ a	1.9(2) d	$1.6(2) \cdot 10^4$ a
	EC/β^+				$2.8(3) \cdot 10^3$ a	1.6(2) d	$1.4(2) \cdot 10^4$ a
^{114}Te $\rightarrow$ ^{114}Sb	EC	$0h_{11/2} - 0f_{5/2}$	$5.03 \cdot 10^{-4}$	$1.24 \cdot 10^{-3}$	9.3(2) a	1.54(3) a	43.7(9) a
	β^+				255(6) a	37.3(9) a	$1.20(3) \cdot 10^3$ a
	EC/β^+				8.9(2) a	1.48(3) a	42(2) a
^{114}Sb $\rightarrow$ ^{114}Sn	EC	$0h_{11/2} - 0f_{5/2}$	$5.77 \cdot 10^{-4}$	$1.25 \cdot 10^{-3}$	118(4) d	25.3(7) d	2.42(5) a
	β^+				39(2) d	8.3(4) d	183(7) d
	EC/β^+				29(2) d	6.2(3) d	136(6) d
^{116}Te $\rightarrow$ ^{116}Sb	EC	$0h_{11/2} - 0f_{5/2}$	$3.30 \cdot 10^{-4}$	$1.25 \cdot 10^{-3}$	521(9) a	36.5(7) a	$2.45(5) \cdot 10^3$ a
	β^+				$1.94(9) \cdot 10^6$ a	$1.36(6) \cdot 10^5$ a	$9.1(4) \cdot 10^6$ a
	EC/β^+				521(9) a	36.5(7) a	$2.45(5) \cdot 10^3$ a
^{116}Sb $\rightarrow$ ^{116}Sn	EC	$0h_{11/2} - 0f_{5/2}$	$6.05 \cdot 10^{-4}$	$1.25 \cdot 10^{-3}$	1.36(2) a	166(2) d	6.39(8) a
	β^+				1.29(3) a	110(2) d	6.1(2) a
	EC/β^+				241(4) d	56.4(9) d	3.10(3) a
^{130}Ce $\rightarrow$ ^{130}La	EC	$0h_{11/2} - 0f_{5/2}$	$5.33 \cdot 10^{-4}$	$1.24 \cdot 10^{-3}$	15.4(3) a	2.85(5) a	72(1) a
	β^+				410(70) a	2.85(2) a	$1.9(3) \cdot 10^3$ a
	EC/β^+				15.2(3) a	2.83(5) a	71(2) a
^{130}La $\rightarrow$ ^{130}Ba	EC	$0h_{11/2} - 0f_{5/2}$	$5.28 \cdot 10^{-4}$	$1.25 \cdot 10^{-3}$	141(2) d	25.0(4) d	1.81(2) a
	β^+				105(2) d	18.6(3) d	1.35(2) a
	EC/β^+				60(1) d	10.7(2) d	282(6) d
^{132}Sn $\rightarrow$ ^{132}Sb	β^-	$0h_{11/2} - 0f_{5/2}$	$1.03 \cdot 10^{-4}$	$1.31 \cdot 10^{-3}$	3(2) a	29(1 mag) d	10(1 mag) a

third significantly lower. The factors k for these three regions for each degree of forbiddeness is listed in table VII. It seems that for the mass region A=50-121 $k \approx 0.41$. In the mass region A=122-146 there is not only a lot of decays with $k < 0.01$ but for the other decays the ratio k is also significantly lower, only around 0.21. However, there were only a handful of group one decay NMEs in the region A=122-146, so the reduction might not be so large with a bigger sample size. The degree of forbiddeness doesn't affect the ratio k within the two groups, but in the higher forbidden decays the proportion of second group decays is much higher.

For most of the semi-magic NMEs in figure 3 the ratio of pnQRPA and two-qp NMEs is approximately 0.0025 with the ratios of ^{54}Fe, ^{88}Sr, ^{90}Zr, ^{114}Sn and ^{116}Sn behaving just like the most of nuclei with $k \approx 0.45$. What makes the tin isotopes interesting, is that the ratio for the isotopes ^{110}Sn and ^{112}Sn is much lower with $k = 0.0006$ and $k = 0.0012$ respectively. In the letter [10] regarding the SD NMEs decays including the semi-magic nuclei ^{86}Kr, ^{88}Sr and ^{122}Sn were included in the study, but the ratios for them did not differ noticeably from the others. From the figure 3 one can see that only one of third of the second and third forbidden semi-magic NMEs and all of the higher forbidden semi-magic NMEs belong to the second group. The higher forbidden decays have therefore more anomaly low NME ratios. There is clearly something different about the heavier and the lighter tin iso-

TABLE III. Computed (partial) half-lives for third forbidden unique β^-, β^+ and EC decays with pnQRPA and two-qp models and the used NMEs. The transitions are $(0+) \leftrightarrow (4-)$, where $(0+)$ is the ground state in the even-even-nucleus of the decay. The expected experimental half-lives are scaled from the pnQRPA half-lives with the scaling factor ξ presented in table VIII.

Transition	Mode	Two-qp	$\lvert M_{\mathrm{pnQRPA}}\rvert$	$\lvert M_{\mathrm{qp}}\rvert$	$t_{1/2(\mathrm{QRPA})}$	$t_{1/2(\mathrm{QP})}$	Expected $t_{1/2}$
^{74}Zn $\rightarrow$ ^{74}Ga	β^-	$0f_{7/2} - 1d_{5/2}$	$4.04 \cdot 10^{-6}$	$8.84 \cdot 10^{-6}$	$1.6(1) \cdot 10^{5}$ a	$3.4(2) \cdot 10^{3}$ a	$3.5(3) \cdot 10^{5}$ a
^{74}Ga $\rightarrow$ ^{74}Ge	β^-	$1p_{3/2} - 1d_{5/2}$	$6.30 \cdot 10^{-6}$	$1.11 \cdot 10^{-5}$	68(3) a	21.7(7) a	150(6) a
^{74}Kr $\rightarrow$ ^{74}Br	EC	$1d_{5/2} - 1p_{3/2}$	$7.27 \cdot 10^{-6}$	$1.38 \cdot 10^{-5}$	$2.08(5) \cdot 10^{5}$ a	$5.8(2) \cdot 10^{4}$ a	$4.6(1) \cdot 10^{5}$ a
	β^+				$2.11(8) \cdot 10^{6}$ a	$5.9(2) \cdot 10^{5}$ a	$4.6(2) \cdot 10^{6}$ a
	EC/β^+				$1.90(5) \cdot 10^{5}$ a	$5.3(2) \cdot 10^{4}$ a	$4.18(9) \cdot 10^{5}$ a
^{74}Br $\rightarrow$ ^{74}Se	EC	$1d_{5/2} - 1p_{3/2}$	$4.70 \cdot 10^{-6}$	$1.43 \cdot 10^{-5}$	2.39(4) a	259(4) a	5.26(8) a
	β^+				167(3) a	18.1(3) a	367(6) a
	EC/β^+				156(3) a	16.9(3) a	343(7) a
^{86}Zr $\rightarrow$ ^{86}Y	EC	$1d_{5/2} - 1p_{3/2}$	$6.18 \cdot 10^{-6}$	$1.54 \cdot 10^{-5}$	$7.9(8) \cdot 10^{7}$ a	$1.3(2) \cdot 10^{7}$ a	$1.7(2) \cdot 10^{8}$ a
	β^+				$1.7(9) \cdot 10^{13}$ a	$3(2) \cdot 10^{12}$ a	$3(2) \cdot 10^{13}$ a
	EC/β^+				$7.9(8) \cdot 10^{7}$ a	$1.3(2) \cdot 10^{7}$ a	$1.8(2) \cdot 10^{8}$ a
^{86}Y $\rightarrow$ ^{86}Sr	EC	$1d_{5/2} - 1p_{3/2}$	$9.04 \cdot 10^{-6}$	$1.55 \cdot 10^{-5}$	$5.2(2) \cdot 10^{3}$ a	$1.77(5) \cdot 10^{3}$ a	$1.1(4) \cdot 10^{4}$ a
	β^+				$2.11(8) \cdot 10^{3}$ a	720(30) a	$5(2) \cdot 10^{3}$ a
	EC/β^+				$1.50(5) \cdot 10^{3}$ a	510(20) a	$3.3(1) \cdot 10^{3}$ a
^{88}Mo $\rightarrow$ ^{88}Nb	EC	$1d_{5/2} - 1p_{3/2}$	$6.04 \cdot 10^{-6}$	$1.55 \cdot 10^{-5}$	$2.60(5) \cdot 10^{4}$ a	$3.93(8) \cdot 10^{3}$ a	$5.7(2) \cdot 10^{4}$ a
	β^+				$1.13(3) \cdot 10^{5}$ a	$17.1(5) \cdot 10^{3}$ a	$2.49(7) \cdot 10^{5}$ a
	EC/β^+				$2.12(5) \cdot 10^{4}$ a	$3.20(7) \cdot 10^{3}$ a	$4.7(1) \cdot 10^{4}$ a
^{88}Nb $\rightarrow$ ^{88}Zr	EC	$1d_{5/2} - 1p_{3/2}$	$7.38 \cdot 10^{-6}$	$1.57 \cdot 10^{-5}$	39.3(6) a	8.7(2) a	86(2) a
	β^+				5.00(8) a	1.11(2) a	11.0(2) a
	EC/β^+				4.44(8) a	359(6) d	8.8(2) a
^{88}Zr $\rightarrow$ ^{88}Y	EC	$1d_{5/2} - 1p_{3/2}$	$7.38 \cdot 10^{-6}$	$1.57 \cdot 10^{-5}$	$1.4(1) \cdot 10^{10}$ a	$3.1(3) \cdot 10^{9}$ a	$2.8(3) \cdot 10^{10}$ a
^{88}Y $\rightarrow$ ^{88}Sr	EC	$0h_{11/2} - 0g_{9/2}$	$9.95 \cdot 10^{-6}$	$1.63 \cdot 10^{-5}$	$8.4(3) \cdot 10^{4}$ a	$3.1(1) \cdot 10^{4}$ a	$1.8(6) \cdot 10^{5}$ a
	β^+				$2.1(2) \cdot 10^{5}$ a	$7.9(5) \cdot 10^{4}$ a	$4.6(8) \cdot 10^{5}$ a
	EC/β^+				$6.0(3) \cdot 10^{4}$ a	$2.2(1) \cdot 10^{4}$ a	$1.3(7) \cdot 10^{5}$ a
^{90}Mo $\rightarrow$ ^{90}Nb	EC	$1d_{5/2} - 1p_{3/2}$	$6.89 \cdot 10^{-6}$	$1.58 \cdot 10^{-5}$	$4.7(5) \cdot 10^{5}$ a	$8.9(9) \cdot 10^{4}$ a	$1.03(9) \cdot 10^{6}$ a
	β^+				$2.9(6) \cdot 10^{7}$ a	$6(1) \cdot 10^{6}$ a	$6.4(2) \cdot 10^{7}$ a
	EC/β^+				$4.6(5) \cdot 10^{5}$ a	$8.7(8) \cdot 10^{4}$ a	$1.0(1) \cdot 10^{6}$ a
^{90}Nb $\rightarrow$ ^{90}Zr	EC	$0h_{11/2} - 0g_{9/2}$	$8.60 \cdot 10^{-6}$	$1.65 \cdot 10^{-5}$	131(5) a	36(2) a	288(9) a
	β^+				31(2) a	8.4(5) a	68(5) a
	EC/β^+				25(2) a	6.8(4) a	55(4) a
^{146}Gd $\rightarrow$ ^{146}Eu	EC	$1d_{3/2} - 0h_{11/2}$	$6.34 \cdot 10^{-8}$	$2.54 \cdot 10^{-5}$	$1.1(1) \cdot 10^{12}$ a	$7.0(7) \cdot 10^{6}$ a	$1.6(2) \cdot 10^{12}$ a
	β^+				$3.2(3) \cdot 10^{26}$ a	$2.2(2) \cdot 10^{21}$ a	$3.2(3) \cdot 10^{26}$ a
	EC/β^+				$1.1(1) \cdot 10^{12}$ a	$7.0(7) \cdot 10^{6}$ a	$1.1(1) \cdot 10^{12}$ a
^{146}Eu $\rightarrow$ ^{146}Sm	EC	$1d_{3/2} - 0h_{11/2}$	$7.32 \cdot 10^{-6}$	$2.57 \cdot 10^{-5}$	$1.44(3) \cdot 10^{4}$ a	$1.16(2) \cdot 10^{3}$ a	$2.16(5) \cdot 10^{4}$ a
	β^+				$2.28(6) \cdot 10^{5}$ a	$18.4(5) \cdot 10^{3}$ a	$3.42(9) \cdot 10^{5}$ a
	EC/β^+				$1.35(3) \cdot 10^{4}$ a	$1.09(2) \cdot 10^{3}$ a	$2.02(5) \cdot 10^{4}$ a

topes. The reasons behind it might explain why the ratio k for the NMEs of semi-magic nuclei is significantly low for about two thirds of the decays studied here, while for one third $k \approx 0.45$. A good hypothesis would be that the configuration in the ground state in the lighter and heavier tin isotopes is different, and that the differences in BCS-based occupation and unoccupation amplitudes are behind the two-magnitude difference.

It turns out that the NME is very sensitive to the single-particle energies. The single-particle energy of the proton orbital 0h11/2 was varied and the pnQRPA calculation was performed for each single-particle value. The results are presented in figure 3. The behavior seems to be similar at low energies, but there is a critical point at -3.75 MeV, at which the pnQRPA NME of ^{114}Sn rises by two magnitudes. For energies higher than -3.75 MeV the NME is almost constant.

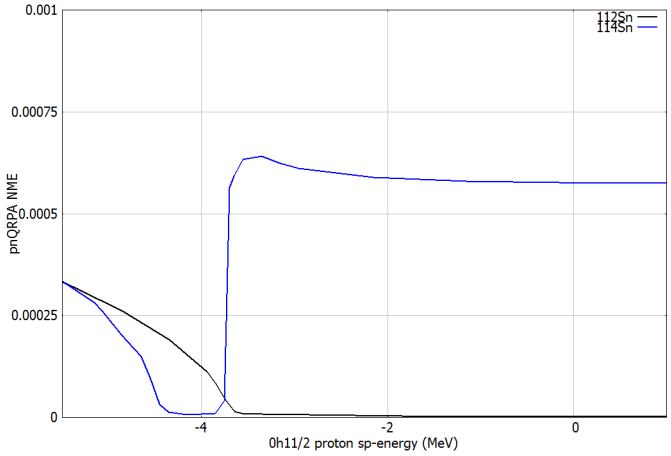

FIG. 5. The NME given by pnQRPA as a function of the single-particle energy of the 0h11/2 proton orbital for ^{112}Sn and ^{114}Sn.

TABLE IV. Computed (partial) half-lives for fourth forbidden unique β^-, β^+ and EC decays with pnQRPA and two-qp models and the used NMEs. The transitions are $(0+) \leftrightarrow (5+)$, where $(0+)$ is the ground state in the even-even-nucleus of the decay. The expected experimental half-lives are scaled from the pnQRPA half-lives with the scaling factor ξ presented in table VIII.

Transition	Mode	Two-qp	$\lvert M_{\rm pnQRPA}\rvert$	$\lvert M_{\rm qp}\rvert$	$t_{1/2({\rm QRPA})}$	$t_{1/2({\rm QP})}$	Expected $t_{1/2}$
^{50}Sc $\rightarrow$ ^{50}Ti	β^-	$1s_{1/2} - 0g_{9/2}$	$7.55 \cdot 10^{-8}$	$1.48 \cdot 10^{-7}$	$4.2(2) \cdot 10^{4}$ a	$1.01(4) \cdot 10^{4}$ a	$9.2(3) \cdot 10^{4}$ a
^{60}Fe $\rightarrow$ ^{60}Co	β^-	$1s_{1/2} - 0g_{9/2}$	$7.23 \cdot 10^{-8}$	$1.62 \cdot 10^{-7}$	$9(1) \cdot 10^{18}$ a	$1.8(2) \cdot 10^{18}$ a	$2.0(3) \cdot 10^{19}$ a
^{60}Co $\rightarrow$ ^{60}Ni	β^-	$1s_{1/2} - 0g_{9/2}$	$5.30 \cdot 10^{-10}$	$1.64 \cdot 10^{-7}$	$2.9(4) \cdot 10^{13}$ a	$3.0(5) \cdot 10^{8}$ a	$6.4(7) \cdot 10^{13}$ a
^{98}Pd $\rightarrow$ ^{98}Rh	EC	$0h_{11/2} - 1p_{1/2}$	$6.55 \cdot 10^{-8}$	$3.21 \cdot 10^{-7}$	$1.6(2) \cdot 10^{11}$ a	$7.1(6) \cdot 10^{9}$ a	$7.5(9) \cdot 10^{11}$ a
	β^+				$6(1) \cdot 10^{14}$ a	$2.7(5) \cdot 10^{13}$ a	$2.8(5) \cdot 10^{15}$ a
	EC/β^+				$1.6(2) \cdot 10^{11}$ a	$7.1(6) \cdot 10^{9}$ a	$7.5(8) \cdot 10^{11}$ a
^{98}Rh $\rightarrow$ ^{98}Ru	EC	$0h_{11/2} - 1p_{1/2}$	$1.20 \cdot 10^{-7}$	$3.20 \cdot 10^{-7}$	$2.40(6) \cdot 10^{7}$ a	$3.40(8) \cdot 10^{6}$ a	$1.13(3) \cdot 10^{8}$ a
	β^+				$4.5(2) \cdot 10^{7}$ a	$6.4(2) \cdot 10^{6}$ a	$2.12(6) \cdot 10^{8}$ a
	EC/β^+				$1.57(5) \cdot 10^{7}$ a	$2.22(6) \cdot 10^{6}$ a	$7.4(3) \cdot 10^{7}$ a
^{102}Cd $\rightarrow$ ^{102}Ag	EC	$0h_{11/2} - 1p_{1/2}$	$6.40 \cdot 10^{-8}$	$3.28 \cdot 10^{-7}$	$5.2(2) \cdot 10^{9}$ a	$2.0(7) \cdot 10^{8}$ a	$2.4(6) \cdot 10^{10}$ a
	β^+				$8.1(5) \cdot 10^{11}$ a	$3.1(2) \cdot 10^{10}$ a	$3.8(2) \cdot 10^{12}$ a
	EC/β^+				$5.2(2) \cdot 10^{9}$ a	$2.0(7) \cdot 10^{8}$ a	$2.4(8) \cdot 10^{10}$ a
^{102}Ag $\rightarrow$ ^{102}Pd	EC	$1d_{5/2} - 1d_{5/2}$	$1.16 \cdot 10^{-7}$	$3.48 \cdot 10^{-7}$	$6.8(2) \cdot 10^{6}$ a	$7.5(2) \cdot 10^{5}$ a	$3.2(7) \cdot 10^{7}$ a
	β^+				$8.9(3) \cdot 10^{6}$ a	$9.8(3) \cdot 10^{5}$ a	$4.2(2) \cdot 10^{7}$ a
	EC/β^+				$3.84(9) \cdot 10^{6}$ a	$4.2(1) \cdot 10^{5}$ a	$1.8(4) \cdot 10^{7}$ a
^{104}Cd $\rightarrow$ ^{104}Ag	EC	$1d_{5/2} - 1d_{5/2}$	$7.68 \cdot 10^{-8}$	$3.47 \cdot 10^{-7}$	$1.43(7) \cdot 10^{13}$ a	$7.0(3) \cdot 10^{11}$ a	$6.7(3) \cdot 10^{13}$ a
	β^+				$3(2) \cdot 10^{22}$ a	$1.3(7) \cdot 10^{21}$ a	$1.4(9) \cdot 10^{23}$ a
	EC/β^+				$1.43(7) \cdot 10^{13}$ a	$7.0(4) \cdot 10^{11}$ a	$6.7(3) \cdot 10^{13}$ a
^{104}Ag $\rightarrow$ ^{104}Pd	EC	$1d_{5/2} - 1d_{5/2}$	$1.40 \cdot 10^{-7}$	$3.79 \cdot 10^{-7}$	$8.0(2) \cdot 10^{7}$ a	$1.76(3) \cdot 10^{7}$ a	$3.8(5) \cdot 10^{8}$ a
	β^+				$4.28(9) \cdot 10^{8}$ a	$9.4(2) \cdot 10^{7}$ a	$2.0(5) \cdot 10^{9}$ a
	EC/β^+				$6.8(2) \cdot 10^{7}$ a	$1.48(3) \cdot 10^{7}$ a	$3.2(6) \cdot 10^{8}$ a
^{130}I $\rightarrow$ ^{130}Te	EC	$1d_{5/2} - 1d_{5/2}$	$2.45 \cdot 10^{-8}$	$4.85 \cdot 10^{-7}$	$5.3(5) \cdot 10^{19}$ a	$1.4(2) \cdot 10^{17}$ a	$2.5(3) \cdot 10^{20}$ a
^{130}I $\rightarrow$ ^{130}Xe	β^-	$1p_{3/2} - 1f_{7/2}$	$4.60 \cdot 10^{-9}$	$3.96 \cdot 10^{-7}$	$1.03(2) \cdot 10^{11}$ a	$1.39(3) \cdot 10^{7}$ a	$4.84(6) \cdot 10^{11}$ a
^{136}Cs $\rightarrow$ ^{136}Xe	EC	$1d_{5/2} - 1d_{5/2}$	$1.39 \cdot 10^{-9}$	$4.81 \cdot 10^{-7}$	$1(2\ {\rm mag}) \cdot 10^{31}$ a	$1.1(2\ {\rm mag}) \cdot 10^{26}$ a	$5(2\ {\rm mag}) \cdot 10^{31}$ a
^{136}Cs $\rightarrow$ ^{136}Ba	β^-	$1p_{3/2} - 1f_{7/2}$	$3.40 \cdot 10^{-9}$	$4.07 \cdot 10^{-7}$	$9.1(8) \cdot 10^{11}$ a	$6.4(6) \cdot 10^{7}$ a	$4.3(4) \cdot 10^{12}$ a
^{138}La $\rightarrow$ ^{138}Ba	EC	$0h_{11/2} - 0h_{11/2}$	$1.09 \cdot 10^{-9}$	$4.68 \cdot 10^{-7}$	$6.0(2) \cdot 10^{15}$ a	$3.28(8) \cdot 10^{10}$ a	$9.0(3) \cdot 10^{15}$ a
	β^+				$1.47(7) \cdot 10^{20}$ a	$8.0(4) \cdot 10^{14}$ a	$2.2(1) \cdot 10^{20}$ a
	EC/β^+				$6.0(2) \cdot 10^{15}$ a	$3.28(8) \cdot 10^{10}$ a	$9.0(3) \cdot 10^{15}$ a
^{138}La $\rightarrow$ ^{138}Ce	β^-	$1p_{1/2} - 1f_{7/2}$	$4.41 \cdot 10^{-9}$	$4.10 \cdot 10^{-7}$	$7.4(8) \cdot 10^{15}$ a	$8.5(9) \cdot 10^{11}$ a	$1.1(2) \cdot 10^{16}$ a

TABLE VII. The ratio $k = M_{\rm pnQRPA}/M_{\rm qp}$ as a function of mass number A and degree of forbiddeness K for decays with $k > 0.01$.

A	$K=2$	$K=3$	$K=4$	$K=6$	Avg.
50-88	0.36	0.48	0.48	-	0.44
89-121	0.37	0.48	0.28	0.43	0.39
122-150	0.31	0.28	0.05	-	0.21

The critical point was found to be the single-particle energy at which the ground-state configuration changes from the 0h11/2-0h11/2 dominated of the lower energies to the 1d5/2-2s1/2 dominated of the higher 0h11/2 proton orbital energies. The energies of the proton orbital calculated from the Woods-Saxon potential were 0.67 MeV and -0.15 MeV for the ^{112}Sn and ^{114}Sn isotopes respectively, which are on the far right side of the critical point. In the ^{122}Sn isotope these orbitals are in the same order as in the ^{114}Sn isotope resulting in a pnQRPA NME which is relatively large.

The average of the ratios of the pnQRPA and two-qp NMEs of the first group agrees with the value given for GT decays in [11]. The decays with $k < 0.01$ seem to be more of a higher forbiddeness phenomenon. A good guess would be that the ratio $k_{\rm NM} = M^m_{\rm exp}/M^m_{\rm pnQRPA}$ is also approximately the same as in [11]. The ratio $k_{\rm NM}$ was listed as a function the qp n − p configuration for the GT decays. However, this does not include all the configurations in the present calculations, so we will just list the value of $k_{\rm NM}$ approximately for different mass regions. The ratio $k_{\rm NM}$ is listed in table VIII along with the factor $\xi = (k_{\rm NM})^{-2} = t_{1/2\ {\rm exp}}/t_{1/2\ {\rm pnQRPA}}$ in which we are really interested in. The factor ξ was used to calculate the expected experimental values in tables II-VI.

TABLE VIII. The ratio $k_{\rm NM} = M^m_{\rm exp}/M^m_{\rm pnQRPA}$ and the factor $\xi = (k_{\rm NM})^{-2} = t_{1/2\ {\rm exp}}/t_{1/2\ {\rm pnQRPA}}$ for different mass regions based on the results in [11].

A	$k_{\rm NM}$	ξ
50-96	0.67	2.2
98-136	0.46	4.7
138-146	0.82	1.5

TABLE V. Computed (partial) half-lives for sixth forbidden unique β^-, β^+ and EC decays with pnQRPA and two-qp models and the used NMEs. The transitions are $(0+) \leftrightarrow (7+)$, where $(0+)$ is the ground state in the even-even-nucleus of the decay. The expected experimental half-lives are scaled from the pnQRPA half-lives with the scaling factor ξ presented in table VIII.

Transition	Mode	Two-qp	$\lvert M_{\rm pnQRPA}\rvert$	$\lvert M_{\rm qp}\rvert$	$t_{1/2({\rm QRPA})}$	$t_{1/2({\rm QP})}$	Expected $t_{1/2}$
^{92}Nb $\rightarrow$ ^{92}Zr	EC	$1d_{5/2} - 0g_{9/2}$	$6.96 \cdot 10^{-11}$	$1.57 \cdot 10^{-10}$	$4.2(6) \cdot 10^{19}$ a	$8(2) \cdot 10^{18}$ a	$9(2) \cdot 10^{19}$ a
	β^+				$1.0(3) \cdot 10^{24}$ a	$2.0(6) \cdot 10^{23}$ a	$2.2(5) \cdot 10^{24}$ a
	EC/β^+				$4.2(6) \cdot 10^{19}$ a	$8.4(2) \cdot 10^{18}$ a	$9(2) \cdot 10^{19}$ a
^{92}Nb $\rightarrow$ ^{92}Mo	β^-	$1p_{3/2} - 0h_{11/2}$	$8.53 \cdot 10^{-11}$	$1.43 \cdot 10^{-10}$	$2(1\ {\rm mag}) \cdot 10^{28}$ a	$7(1\ {\rm mag}) \cdot 10^{27}$ a	$4(1\ {\rm mag}) \cdot 10^{28}$ a
^{94}Ru $\rightarrow$ ^{94}Tc	EC	$1d_{5/2} - 0g_{9/2}$	$5.20 \cdot 10^{-13}$	$1.61 \cdot 10^{-10}$	$1.25(1) \cdot 10^{25}$ a	$1.3(2) \cdot 10^{19}$ a	$2.75(3) \cdot 10^{25}$ a
	β^+				$2.20(4) \cdot 10^{31}$ a	$2.3(4) \cdot 10^{25}$ a	$4.84(8) \cdot 10^{31}$ a
	EC/β^+				$1.25(1) \cdot 10^{25}$ a	$1.3(2) \cdot 10^{19}$ a	$2.75(3) \cdot 10^{25}$ a
^{94}Tc $\rightarrow$ ^{94}Mo	EC	$1d_{5/2} - 0g_{9/2}$	$6.03 \cdot 10^{-11}$	$1.59 \cdot 10^{-10}$	$1.16(3) \cdot 10^{15}$ a	$1.67(3) \cdot 10^{14}$ a	$2.55(6) \cdot 10^{15}$ a
	β^+				$4.7(1) \cdot 10^{16}$ a	$6.7(2) \cdot 10^{15}$ a	$1.0(2) \cdot 10^{17}$ a
	EC/β^+				$1.14(3) \cdot 10^{15}$ a	$1.63(4) \cdot 10^{14}$ a	$2.51(7) \cdot 10^{15}$ a
^{96}Tc $\rightarrow$ ^{96}Mo	EC	$1d_{5/2} - 0g_{9/2}$	$8.47 \cdot 10^{-11}$	$1.62 \cdot 10^{-10}$	$9.3(3) \cdot 10^{16}$ a	$2.55(7) \cdot 10^{16}$ a	$2.0(6) \cdot 10^{17}$ a
	β^+				$4.7(2) \cdot 10^{19}$ a	$1.27(6) \cdot 10^{19}$ a	$1.03(3) \cdot 10^{20}$ a
	EC/β^+				$5.3(3) \cdot 10^{16}$ a	$2.55(7) \cdot 10^{16}$ a	$1.17(6) \cdot 10^{17}$ a
^{96}Tc $\rightarrow$ ^{96}Ru	β^-	$1p_{3/2} - 0h_{11/2}$	$8.88 \cdot 10^{-11}$	$1.49 \cdot 10^{-10}$	$5.4(2) \cdot 10^{29}$ a	$1.9(5) \cdot 10^{29}$ a	$1.19(9) \cdot 10^{30}$ a
^{108}Sn $\rightarrow$ ^{108}In	EC	$1d_{5/2} - 0g_{9/2}$	$2.52 \cdot 10^{-13}$	$1.79 \cdot 10^{-10}$	$8.1(9) \cdot 10^{22}$ a	$1.6(2) \cdot 10^{17}$ a	$3.8(4) \cdot 10^{23}$ a
	β^+				$3.3(6) \cdot 10^{27}$ a	$6(1) \cdot 10^{21}$ a	$1.6(3) \cdot 10^{28}$ a
	EC/β^+				$8.1(9) \cdot 10^{22}$ a	$1.6(2) \cdot 10^{17}$ a	$3.8(4) \cdot 10^{23}$ a
^{108}In $\rightarrow$ ^{108}Cd	EC	$1d_{5/2} - 0g_{9/2}$	$6.05 \cdot 10^{-11}$	$1.79 \cdot 10^{-10}$	$5.1(2) \cdot 10^{13}$ a	$5.9(2) \cdot 10^{12}$ a	$2.4(7) \cdot 10^{14}$ a
	β^+				$1.27(5) \cdot 10^{15}$ a	$1.45(6) \cdot 10^{14}$ a	$6.0(2) \cdot 10^{15}$ a
	EC/β^+				$4.9(2) \cdot 10^{13}$ a	$5.7(2) \cdot 10^{12}$ a	$2.3(6) \cdot 10^{14}$ a
^{110}Sn $\rightarrow$ ^{110}In	EC	$1d_{5/2} - 0g_{9/2}$	$2.55 \cdot 10^{-13}$	$1.82 \cdot 10^{-10}$	$2(1) \cdot 10^{30}$ a	$4(2) \cdot 10^{24}$ a	$9(5) \cdot 10^{30}$ a
^{110}In $\rightarrow$ ^{110}Cd	EC	$1d_{5/2} - 0g_{9/2}$	$6.45 \cdot 10^{-11}$	$1.82 \cdot 10^{-10}$	$2.4(1) \cdot 10^{15}$ a	$3.0(2) \cdot 10^{14}$ a	$1.1(5) \cdot 10^{16}$ a
	β^+				$3.5(2) \cdot 10^{17}$ a	$3.8(3) \cdot 10^{16}$ a	$1.6(6) \cdot 10^{18}$ a
	EC/β^+				$2.3(1) \cdot 10^{15}$ a	$3.0(2) \cdot 10^{14}$ a	$1.1(5) \cdot 10^{16}$ a

TABLE VI. Computed (partial) half-lives for seventh forbidden unique β^-, β^+ and EC decays with pnQRPA and two-qp models and the used NMEs. The transitions are $(0+) \leftrightarrow (8-)$, where $(0+)$ is the ground state in the even-even-nucleus of the decay. The expected experimental half-lives are scaled from the pnQRPA half-lives with the scaling factor ξ presented in table VIII.

Transition	Mode	Two-qp	$\lvert M_{\rm pnQRPA}\rvert$	$\lvert M_{\rm qp}\rvert$	$t_{1/2({\rm QRPA})}$	$t_{1/2({\rm QP})}$	Expected $t_{1/2}$
^{126}Sn $\rightarrow$ ^{126}Sb	β^-	$0g_{9/2} - 1f_{7/2}$	$6.12 \cdot 10^{-15}$	$5.53 \cdot 10^{-12}$	$1.9(2) \cdot 10^{20}$ a	$2.4(2) \cdot 10^{14}$ a	$8.9(8) \cdot 10^{20}$ a
^{132}Sn $\rightarrow$ ^{132}Sb	β^-	$0g_{9/2} - 1f_{7/2}$	$8.66 \cdot 10^{-18}$	$5.84 \cdot 10^{-12}$	$3.4(4) \cdot 10^{27}$ a	$7.4(6) \cdot 10^{14}$ a	$1.6(2) \cdot 10^{28}$ a

V. CONCLUSIONS

The decays are divided into two groups where the ratio of the pnQRPA and two-qp NMEs is about 0.25-0.6 for the first group and less than 0.01 for the second group. About 4/5 of all decays belong to the first group. Majority of the non-magic and second and third forbidden decays including a semi-magic nuclei belong to the first group, where as majority of the semi-magic higher forbidden NMEs belong to the second group. The mean pnQRPA NMEs $M^m_{\rm pnQRPA}$ of the nuclei in the first group were determined to be reduced by a factor of $k = 0.41 \pm 0.12$ with respect to the two-qp NMEs. This is due to the spin-isospin correlation which is taken into account in pnQRPA but not the two-qp model [10, 11]. The value of k was found to be reduced to 0.21 for the mass region 122-146. The average reduction factor is in good agreement with the values for the Gamow-Teller and spin-dipole matrix elements of the earlier studies. The dependence on A is how ever different. Since the transition from two-qp to pnQRPA affects the highly forbidden unique NMEs roughly the same way as the SD and GT NMEs, the difference of the pnQRPA and the observed matrix elements is most likely also similar. This means that the pnQRPA NMEs are reduced by 1.5-4.7 depending on the mass number [11].

The difference between the pnQRPA and observed half-lives is due to nuclear medium effects, and so although the pnQRPA NMEs are reduced by many magnitudes with respect to the two-qp NMEs, the difference between the experimental and pnQRPA half-lives should still be similar.

The reduction factor k seems to depend on the degree of forbiddenss. The proportion of $k < 0.01$ NMEs is greater for more highly forbidden decays. For mass regions 50-88, 90-121 and 122-146 the factor k is approximately 0.44, 0.39 or 0.21 respectively, or then it is ex-

tremely low with $k < 0.01$. The reduction factor is dependent on whether the even-even nucleus is magic or not. 95 % of the decays with non-magic even-even nucleus belong to the first group while only 30 % of the decays with a semi-magic even-even nucleus do. The NME of the semi-magic nucleus is heavily dependent on the single-particle energies, and a slight change might alter it by magnitudes. The dependence of the NME on the single-particle energy is not exclusive to the semi-magic nuclei, but is manifested more heavily, since the BCS-calculation gives a rather sharp Fermi-surface, and the occupation and unoccupation amplitudes are close to 1 and 0.

The ratio of the mean NMEs does not seem to be affected by whether the mean is taken from two NMEs with a common mother or daughter nucleus or just from NMEs with the same A. The variance wasn't significantly low in either case, and the observed low variance of the SD NMEs in the letter [10] might be partially caused by the small sample size.

[1] H. Behrens and W. Bühring, *Electron Radial Wave Functions and Nuclear Beta Decay* (Clarendon, Oxford, 1982).
[2] M. Haaranen, M. Horoi, and J. Suhonen, Phys. Rev. C **89**, 034315 (2014).
[3] M. T. Mustonen, M. Aunola, and J. Suhonen, Phys. Rev. C **73**, 054301 (2006).
[4] M. Aunola, J. Suhonen, and T. Siiskonen, Europhys. Lett. **46**, 577 (1999).
[5] E. K. Warburton, Phys. Rev. C **31**, 1898 (1985).
[6] J. S. E. W. *et al.*, Phys. Rev. Lett. **103**, 122501 (2009).
[7] M. T. Mustonen and J. Suhonen, J. Phys. G **37**, 064008 (2010).
[8] M. T. Mustonen and J. Suhonen, Phys. Lett. B **703**, 370 (2011).
[9] M. Haaranen and J. Suhonen, Eur. Phys J. A **19**, 93 (2013).
[10] H. Ejiri, N. Soukouti, and J. Suhonen, Phys. Lett. B **729**, 27 (2014).
[11] H. Ejiri and J. Suhonen, J. Phys. G: Nucl. Part. Phys. **42**, 055201 (2015).
[12] L. Jokiniemi, J. Suhonen, and H. Ejiri, Adv. High Energ. Phys. **88**, 8417598 (2016).
[13] J. Suhonen, *From Nucleons to Nucleus: Concepts of Microscopic Nuclear Theory* (Springer, Berlin, 2007).
[14] H. Ejiri, Phys. Rep. **338**, 265 (2000).
[15] J. Vergados, H. Ejiri, and F. Šimkovic, Rep. Prog. Phys. **75**, 106301 (2012).
[16] S. R. Elliott and P. Vogel, Annu. Rev. Nucl. Part. Sci. **52**, 115 (2005).
[17] H. Ejiri, J. Phys. Soc. Jpn. **74**, 2101 (2005).
[18] F. Avignone, S. Elliott, and J. Engel, Rev. Mod. Phys. **80**, 481 (2008).
[19] J. Suhonen and O. Civitarese, Phys. Rep. **300**, 123 (1998).
[20] M. Haaranen, P. C. Srivastava, and J. Suhonen, Phys. Rev. C **93**, 034308 (2016).
[21] J. Suhonen and O. Civitarese, Phys. Lett. B **725**, 153 (2013).
[22] J. Suhonen and O. Civitarese, Nucl. Phys. A **924**, 1 (2014).
[23] J. Suhonen and O. Civitarese, J. Phys. G: Nucl Part. Phys. **39**, 085105 (2012).
[24] J. C. Hardy, I. S. Towner, V. Koslowsky, E. Hagberg, and H. Schmeing, Nucl. Phys. A **509**, 429 (1990).
[25] H. Primakoff and S. P. Rosen, Rep. Prog Phys. **22**, 121 (1959).
[26] N. B. Gove and M. Martin, Atom. Data and Nuc. Data Tabl. **10**, 205 (1971).
[27] E. Ydrefors, M. T. Mustonen, and J. Suhonen, Nucl. Phys. A **842**, 33 (2010).
[28] H. Heiskanen, M. T. Mustonen, and J. Suhonen, J. Phys. G: Nucl. Part. Phys. **34**, 837–843 (2007).
[29] J. Suhonen, Nucl. Phys. A **563**, 205 (1993).
[30] National Nuclear Data Center, Brookhaven National Laboratory, `www.nndc.bnl.gov`.

FYSZ490 Pro Gradu -liite

Joel Kostensalo

1 Johdanto

Tämän liitteen tarkoituksena on selventää tulosten saamiseen käytettyjä menetelmiä Pro Gradussani *Half-lives for Highly Forbidden Unique Beta Decays in Medium-heavy Nuclei*. Koska kyseinen tutkielma on kirjoitettu tieteellisen artikkelin muotoon, on joitain tulosten saamiseen liittyviä yksityiskohtia jouduttu jättämään pituuden vuoksi pois. Tavoitteena on saada julkaistua tutkielma korjausehdotusten mukaisesti muokattuna kansainvälisessä lehdessä, jonka kohdeyleisönä ovat alan tutkijat. Opinnäytetyö pyritään yleensä kirjoittamaan ajatellen lukijan esitietojen olevan samaa tasoa kuin aiheeseen erikseen perehtymättömällä opiskelijalla. Kohdeyleisöstä johtuen tutkielmassa on sivuutettu lyhyellä maininnalla joitain asioita, joita olisi perinteisessä Pro Gradussa voitu tarkastella yksityiskohtaisemmin.

Tutkielman aiheeseen liittyvää teoriaa on käsitelty ymmärtämisen kannalta tarpeeksi tutkielmassa, ja tarkempia yksityiskohtia varten on viitattu kirjallisuuteen. Seuraavissa kahdessa luvussa tullaan käsittelemään sitä, miten tuloksiin käytännössä päädyttiin. Luvussa 2 esitellään, miten β-hajoamisten puoliintumisaikojen laskeminen käytännössä toteutettiin, ja luvussa 3 käydään läpi tulosten käsittelyyn liittyviä menetelmiä. Luvussa 3 on esitelty erityisesti, miten tulosten analysoimisessa päädyttiin tutkielmassa esiintyviin tarkasteluihin, kuten $0\mathrm{h}_{11/2}$-protoniorbitaalin energian varioimiseen sekä puoli- ja ei-maagisten ydinmatriisielementtien tarkasteluun erikseen. Itse artikkelissa ei ollut järkevää mainita, millaisia epäolennaisiksi osoittautuneita tarkasteluita tehtiin. Lopusta löytyvät liitteet. Liitteistä löytyvät matriisielementit ja faasiavaruusintegraalit virheineen (taulukot 1–5) sekä puoliintumisajat (taulukot 6–10). "Kokeellisten" puoliintumisaikojen epätarkkuuden arviointia on muutettu tähän liitteeseen siten, että myös tekijälle k määritettiin virhe ja sen vaikutus otettiin huomioon.

2 Puoliintumisajan määrittäminen

Kaikki tutkitut siirtymät olivat parillinen–parillinen- ja pariton–pariton-ytimien välisiä. Ydinmatriisielementtien (YME) (tutkielmassa *nuclear matrix element (NME)*) laskemisessa käytettiin referenssiytimenä parillinen–parillinen-ydintä, ja pnQRPA-tyhjiö oli tämän ytimen perustila. YME:ien laskemista varten tarvittiin ensin orbitaalien yksihiukkasenergiat, joita käytettiin BCS-yhtälöiden ratkaisemiseen. Lisäksi siirtymään liittyvä faasiavaruusintegraali laskettiin numeerisesti, minkä jälkeen puoliintumisaika voitiin laskea YME:n ja faasiavaruusintegraalin avulla. Seuraavissa alaluvuissa on käsitelty yksihiukkasenergioiden laskemista, puoliintumisajan ja osittaispuoliintumisaikojen laskua sekä virheanalyysiä.

2.1 Yksihiukkasenergiat

Yksihiukkasenergioiden ratkaisemiseen käytettiin numeerista ohjelmaa, joka laskee protoni- ja neutroniorbitaalien energiat. Potentiaalina käytettiin *Woods–Saxon*-potentiaalia *Bohr–Mottelson*-parametrisaatiolla [1]

$$f(r,R,a) = \left[1 + \exp\left(\frac{r-R}{a}\right)\right]^{-1},$$

missä $a = 0{,}7$ fm on pinnan diffuusioparametri ja $R = r_0 A^{1/3}$ on ytimen säde. Spin-orbitaalipotentiaalille vakio $r_0 = 1.10$ fm. Yksihiukkasenergioiden ratkaisemista varten ohjelmalle syötettiin alkuarvaukset, jotka kertoivat, etsikö ohjelma kullekin orbitaalille sidottua vai ei-sidottua tilaa. Ohjelmalla oli konvergoimisongelmia nollan läheisyydessä, joten laskun tuottaessa selvästi virheellisiä energioita interpoloitiin energia naapuriytimien yksihiukkasenergioista.

2.2 Puoliintumisaika

Kielletyn uniikin beetasiirtymän puoliintumisaika määritettiin käyttäen yhtälöä

$$t_{1/2} = \frac{\kappa}{f \cdot B_{Ku}}, \tag{1}$$

missä f on faasiavaruusintegraali ja B_{Ku} on redusoitu beetasiirtymätodennäköisyys. B_{Ku} voidaan laskea käyttämällä yhtälöä

$$B_{Ku} = \frac{1}{2J_i + 1}|M_{Ku}|, \tag{2}$$

missä J_i on lähtöytimen pyörimismäärä ja M_{Ku} on YME. Tarkennuksia YME:n ja faasiavaruusintegraalin laskemiseen on esitetty alaluvuissa 2.2.1 ja 2.2.2.

2.2.1 Ydinmatriisielementti

YME:ien määrittämiseen käytettiin pnQRPA-teoriaa. YME:n M_{pnQRPA} saamiseksi ratkaistiin numeerisesti pnQRPA-yhtälöt

$$\begin{pmatrix} \mathrm{A} & \mathrm{B} \\ -\mathrm{B}^* & -\mathrm{A}^* \end{pmatrix} \begin{pmatrix} \mathrm{X}^\omega \\ \mathrm{Y}^\omega \end{pmatrix} = E^\omega \begin{pmatrix} \mathrm{X}^\omega \\ \mathrm{Y}^\omega \end{pmatrix} \tag{3}$$

diagonalisoimalla pnQRPA-supermatriisi. Supermatriisissa esiintyvien matriisien A ja B elementtien lausekkeissa esiintyvät miehitysamplitudit u ja v laskettiin ratkaisemalla BCS-yhtälöt numeerisesti iteroimalla. pnQRPA-mallilla ratkaistuja YME:jä (M_{pnQRPA}) verrattiin kaksikvasihiukkasmallilla laskettuihin YME:ihin (M_{qp}). Käsittely valittiin samanlaiseksi kuin Gamow–Teller-hajoamisille ja spin-dipolimatriisielementeille artikkeleissa [2, 3], jotta tuloksia olisi mahdollista verrata aiempiin tuloksiin.

2.2.2 Faasiavaruusintegraali

Faasiavaruusintegraalit laskettiin käyttäen tarkkoja lausekkeita, jotka on esitetty lähteissä [4, 5]. Elektronisieppauksille, joiden Q-arvo oli alle 1022 keV, sekä β^--hajoamisille puoliintumisaika saatiin käyttämällä faasiavaruusintegraalina tekijää $f_{Ku}^{(\mathrm{EC})}$ tai $f_{Ku}^{(-)}$. Hajoamisille, joiden elektronisieppauksen Q-arvo on yli 1022 keV, myös β^+-hajoaminen on mahdollinen. Näissä tapauksissa osittaispuoliintumisajat saatiin käyttämällä yhtälön (1) faasiavaruusintegraalina f tekijää $f_{Ku}^{(\mathrm{EC})}$ tai $f_{Ku}^{(+)}$ ja puoliintumisaika käyttämällä summaa $f = f_{Ku}^{(\mathrm{EC})} + f_{Ku}^{(+)}$.

Faasiavaruusintegraali $f_{K\mathrm{u}}^{(\pm)}$ K-kertaisesti kielletylle uniikille $\beta^{\pm}$-siirtymälle on [4]

$$f_{K\mathrm{u}} = (2K+1)! \int_0^{W_0} W(W_0-W)^2 \sum_{k=1}^{n+1} \frac{\lambda_k p^{2(k-1)} (W_0-W)^{2(n-k+1)}}{(2k-1)![2(n-k+1)+1]!}\, dW, \quad (4)$$

missä $\beta^{\pm}$-siirtymälle $W_0 = Q \mp 1$, p on β-hiukkasen liikemäärä, integroimismuuttuja $W = \sqrt{p^2+1}$ on β-hiukkasen kokonaisenergia ja

$$\lambda_k(Z,W) = \frac{g_{-k}^2 + f_k^2}{2p^2} \left[\frac{(2k-1)!!}{(pR)^{k-1}}\right]^2. \quad (5)$$

Yhtälössä (5) esiintyvät f ja g ovat elektronin/positronin aaltofunktion radiaaliset komponentit ja R ytimen keskimääräinen säde. Elektronisieppauksen faasiavaruusintegraalissa otettiin huomioon vain dominoivat sieppaukset 1s- ja 2s-orbitaaleilta. Elektronisieppauksen faasiavaruusintegraali on 1s- ja 2s-orbitaalien faasiavaruusintegraalien summa $f^{\mathrm{EC}} = f_{1\mathrm{s}}^{\mathrm{EC}} + f_{2\mathrm{s}}^{\mathrm{EC}}$, missä [5]

$$f_x^{\mathrm{EC}} = \frac{1}{2}\beta_x^2 (p_{\nu_x}/m_e c)^2. \quad (6)$$

Yhtälössä (6) esiintyvä orbitaalin x neliöity amplitudi β_x^2 on 1s- ja 2s-orbitaaleille

$$f_{1\mathrm{s}}^{\mathrm{EC}} = (\alpha Z_i)^3 (2\alpha Z_i m_e c R/\hbar)^{2(\gamma_1-1)} \frac{8\gamma_1^2}{\Gamma(1+2\gamma_1)} \quad (7)$$

$$f_{2\mathrm{s}}^{\mathrm{EC}} = (\alpha Z_i)^3 (2\alpha Z_i m_e c R/N\hbar)^{2(\gamma_1-1)} \frac{16\gamma_1^2\Gamma(2+2\gamma_1)}{N^4(N+1)(\Gamma(1+2\gamma_1))^2}, \quad (8)$$

missä α on hienorakennevakio, Z_i lähtöytimen järjestysluku, $N = \sqrt{2(1+\gamma_1)}$ ja $\gamma_1 = \sqrt{1-(\alpha Z_f)^2}$.

Esimerkki 1

Kahdesti kielletylle uniikille β^--hajoamiselle $^{52}\mathrm{Ti}(0^+) \rightarrow {}^{52}\mathrm{V}(3^+)$ hajoamisessa vapautuva energia on $Q_{\beta^-} = 1975(7)$ keV mistä saadaan faasiavaruuskertoimeksi $f_{2u}^{(-)} = 65{,}609$. Ydinmatriisielementiksi saadaan pnQRPA-

laskulla $M_{\text{pnQRPA}} = 1{,}825 \cdot 10^{-4}$, ja suurin kaksihiukkasmatriisielementti on $0d_{3/2}$–$0g_{9/2}$ p–n-konfigu-raatiota vastaava $M_{\text{qp}} = 6{,}678 \cdot 10^{-4}$. Lähtöytimen pyörimismäärä on $J_i = 0$. Puoliintumisajoiksi näillä malleilla saadaan

$$t_{1/2\ \text{pnQRPA}} = \frac{6147\ \text{s}}{f_{2u}^{(-)} \cdot |1{,}25 \cdot M_{\text{pnQRPA}}|^2} \approx 57{,}1\ \text{a}$$

ja

$$t_{1/2\ \text{qp}} = \frac{6147\ \text{s}}{f_{2u}^{(-)} \cdot |1{,}25 \cdot M_{\text{qp}}|^2} \approx 4{,}26\ \text{a}.$$

Skaalaamalla pnQRPA-puoliintumisaikaa tekijällä $\xi = 2{,}2$ saadaan

$$t_{1/2\ \text{exp}} = 2{,}2 \cdot 57{,}1 = 125{,}6\ \text{a}.$$

2.3 Virheanalyysi

Puoliintumisaikojen virheitä arvioitiin käyttäen yleistä virheen etenemislakia. Kokeellinen puoliintumisaika saadaan pnQRPA:lla määritetystä puoliintumisajasta skaalaamalla. Kun tekijöiden k_{NM}, f ja M_{Ku} arvoihin liittyy epätarkkuutta, saadaan "kokeellisen" arvon virheeksi [6]

$$\delta t_{1/2\ \text{exp}} = \sqrt{(\frac{\partial t_{1/2}}{\partial k_{\text{NM}}} \cdot \delta k_{\text{NM}})^2 + (\frac{\partial t_{1/2}}{\partial f} \cdot \delta f)^2 + (\frac{\partial t_{1/2}}{\partial M_{Ku}} \cdot \delta M_{Ku})^2}$$

$$= \sqrt{(\frac{-2\kappa\delta k_{\text{NM}}}{f \cdot \frac{g_{\text{A}}^2}{2J_i+1} k_{\text{NM}}^3 |M_{Ku}|^2})^2 + (\frac{-\kappa\delta f}{f^2 \cdot \frac{g_{\text{A}}^2}{2J_i+1} |k_{\text{NM}} M_{Ku}|^2})^2 + (\frac{-2\kappa\delta M_{Ku}}{f \cdot \frac{g_{\text{A}}^2}{2J_i+1} k_{\text{NM}}^2 |M_{Ku}|^3})^2},$$

ja suhteelliseksi virheeksi

$$\left(\frac{\delta t_{1/2}}{t_{1/2}}\right)_{\text{exp}} = \sqrt{(\frac{-2\delta k_{\text{NM}}}{k_{\text{NM}}})^2 + (-\frac{\delta f}{f})^2 + (-2\frac{\delta M_{Ku}}{M_{Ku}})^2}. \qquad (9)$$

Suhteellinen virhe pnQRPA-puoliintumisajalle saadaan, kun asetetaan $k_{\text{NM}} = 1$, jolloin $\delta k_{\text{NM}} = 0$. Tutkielmassa ei määritetty virhettä kertoimelle k_{NM}, joten "kokeelliselle" puoliintumisajalle käytettiin samaa suhteellista virhettä

kuin pnQRPA-puoliintumisajalle. Kaksikvasihiukkasmallin matriisielementti on eksakti, joten mallin suhteellinen virhe on sama kuin faasiavaruusintegraalin suhteellinen virhe. Gamow–Teller-hajoamisille saatiin artikkelissa [2] tulos $k_{\mathrm{NM}} = 0{,}65 \pm 0{,}15$. Virhe on kohtalaisen suuri, sillä eri orbitaalien k_{NM}-arvot vaihtelevat välillä 0,46–0,82. Tutkielmassa k_{NM} on annettu erikseen eri massa-alueille, ja GT-aineiston perusteella k_{NM}:n epätarkkuuden näillä massa-alueilla voidaan arvioida olevan noin 10 %.

Faasiavaruusintegraalin tarkkuuteen vaikuttaa siirtymässä vapautuvan energian, eli siirtymän Q-arvon, kokeellisen arvon tarkkuus. Faasiavaruusintegraalin suhteelliseksi virheeksi otettiin suurempi suhteista

$$\frac{f(Q+\delta Q)}{f(Q)} - 1 \quad \text{ja} \quad 1 - \frac{f(Q-\delta Q)}{f(Q)},$$

missä $Q \pm \delta Q$ on siirtymässä vapautuva energia virheineen.

YME:ien epätarkkuutta pyrittiin arvioimaan varioimalla skaalauskertoimia g_{pp} ja g_{ph} 10 % oletusarvosta $g_{\mathrm{pp}} = g_{\mathrm{ph}} = 1{,}0$. Molemmista ryhmistä (GROUP 1 ja GROUP 2) valittiin yksi siirtymä, jota vastaavalle YME:lle variointi suoritettiin. Siirtymiksi valittiin $^{92}\mathrm{Nb} \rightarrow {}^{92}\mathrm{Mo}$ ja $^{94}\mathrm{Tc} \rightarrow {}^{94}\mathrm{Ru}$, jotka ovat kuudesti kiellettyjä. Kuvissa 1 ja 2 on esitetty matriisielementin M_{pnQRPA} arvo skaalauskertoimien funktiona. Käytös on lähes täysin lineaarista, ja suurimmat poikkeamat lasketuista arvoista saadaan, kun $g_{\mathrm{pp}} = 0{,}9;\ g_{\mathrm{ph}} = 1{,}1$ ja kun $g_{\mathrm{pp}} = 1{,}1;\ g_{\mathrm{ph}} = 0{,}9$. Tehdyn varioinnin perusteella GROUP 1:lle suhde $\delta M_{\mathrm{pnQRPA}}/M_{\mathrm{pnQRPA}} \approx 0{,}0065$ ja GROUP 2:lle $\delta M_{\mathrm{pnQRPA}}/M_{\mathrm{pnQRPA}} \approx 0{,}038$.

Esimerkki 2

Lasketaan seuraavaksi virhearvio esimerkin 1 siirtymälle. Siirtymä kuuluu GROUP 1:een, joten YME:n epätarkkuus on 0,65 %. Q-arvolla 1968 keV lasketun faasiavaruusintegraalin arvo on 63,848, joten suhteellinen muutos on 2,68 %. Suhteellinen ero faasiavaruusintegraaliin Q-arvolla 1982 keV on hieman pienempi. Virhearvioksi saadaan siis

$$\delta t_{1/2\ \mathrm{exp}} = \sqrt{(-2 \cdot 0{,}1)^2 + (-0{,}0268)^2 + (-2 \cdot 0{,}0065)^2} = 0{,}202;$$

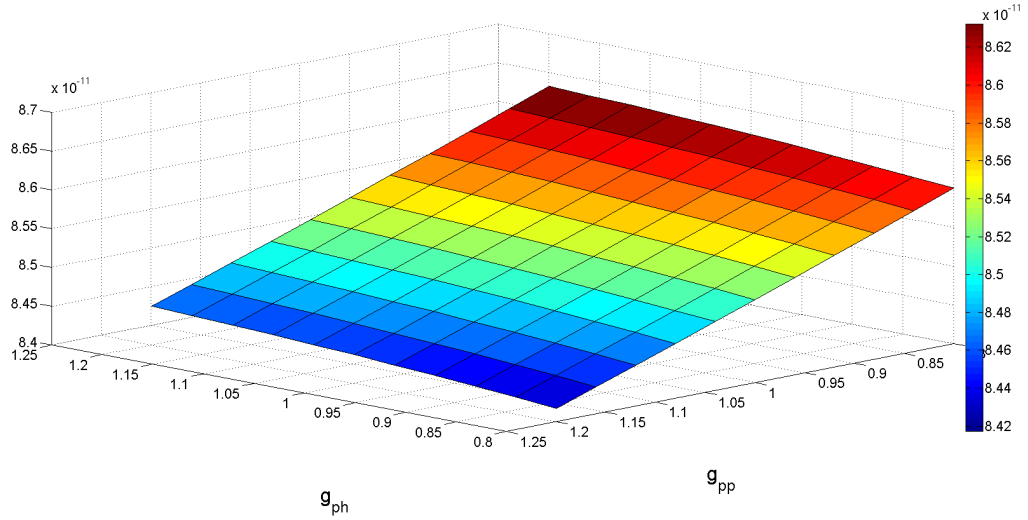

Kuva 1: GROUP 1:een kuuluvan ^{92}Nb $\rightarrow$ ^{92}Mo -ydinmatriisielementin käytös hiukkas–hiukkas- ja hiukkas–aukko-vuorovaikutusparametrien g_{pp} ja g_{ph} funktiona.

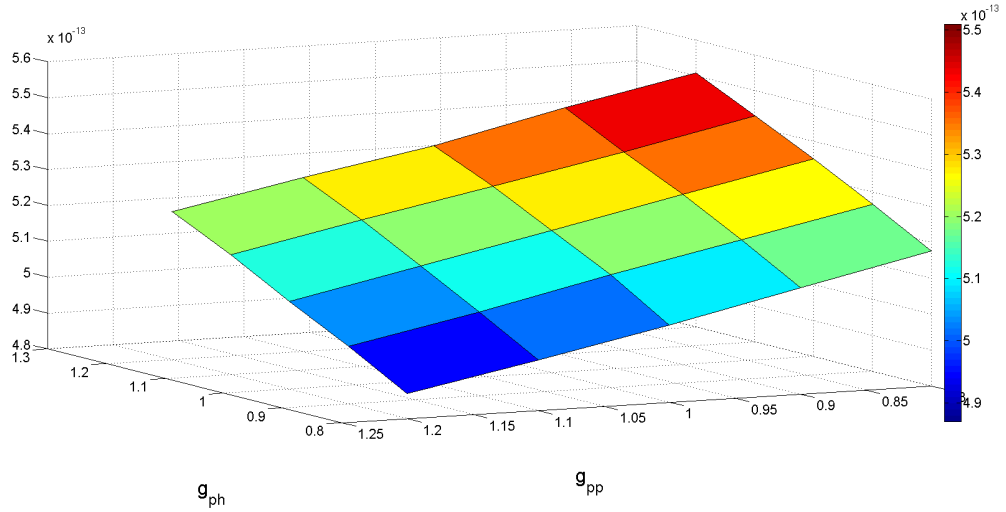

Kuva 2: GROUP 2:een kuuluvan ^{94}Tc $\rightarrow$ ^{94}Ru -ydinmatriisielementin käytös hiukkas–hiukkas- ja hiukkas–aukko-vuorovaikutusparametrien g_{pp} ja g_{ph} funktiona.

$$\delta t_{1/2\ \mathrm{pnQRPA}} = \sqrt{(-0{,}0268)^2 + (-2 \cdot 0{,}065)^2} = 0{,}030.$$

Puoliintumisaikojen virheiksi saadaan siis

$$\begin{aligned} \delta t_{1/2\ \mathrm{pnQRPA}} &= 0{,}030 \cdot 57{,}1\ \mathrm{a} = 1{,}70\ \mathrm{a}, \\ \delta t_{1/2\ \mathrm{qp}} &= 0{,}027 \cdot 4{,}26\ \mathrm{a} = 0{,}115\ \mathrm{a}, \\ \delta t_{1/2\ \mathrm{exp}} &= 0{,}202 \cdot 125{,}6\ \mathrm{a} = 25{,}4\ \mathrm{a}. \end{aligned}$$

Virheet pyöristetään ylöspäin, jolloin saadaan tulokset

$$\begin{aligned} t_{1/2\ \mathrm{pnQRPA}} &= 57(2)\ \mathrm{a}, \\ t_{1/2\ \mathrm{qp}} &= 4{,}3(2)\ \mathrm{a}, \\ t_{1/2\ \mathrm{exp}} &= 1{,}3(3) \cdot 10^2\ \mathrm{a}. \end{aligned}$$

2.4 Tulokset

Tutkielmassa ei listattu pnQRPA-matriisielementtien virheitä eikä faasiavaruusintegraalien arvoja. Nämä on listattu liitteissä taulukoihin 1–5. Liitteistä löytyvät myös puoliintumisajat virheineen taulukoista 6–10. Arvioitujen "kokeellisten" puoliintumisaikojen virheissä on näissä taulukoissa käytetty k_{NM}:n epätarkkuutena 10 %:a, joten arvioitujen puoliintumisaikojen epätarkkuudet ovat vähintään 20 %.

3 Tulosten käsittely

Mahdollisten kokeellisten puoliintumisaikojen ennustamiseksi tutkittiin pnQRPA- ja kaksikvasihiukkasmallien antamien YME:ien arvojen eroja aiempiin tutkimuksiin [2, 3]. Näissä tutkimuksissa on käytetty β^+- ja β^--siirtymien YME:ien geometrista keskiarvoa. Laskettujen YME:ien geometristen keskiarvojen suhteet $\prod_{i=1}^{n}(M_{i(\mathrm{pnQRPA})}/M_{i(\mathrm{qp})})$ on esitetty kuvassa 3 kullekin massaluvulle A. Ne massaluvut, joille oli laskettu korkeintaan yksi YME, jätettiin pois tarkastelusta.

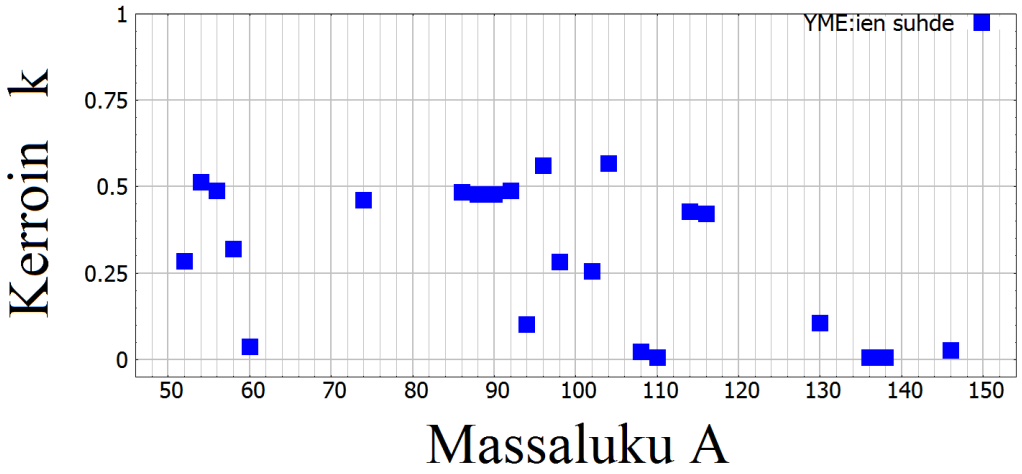

Kuva 3: Suhde $k = M_{\mathrm{pnQRPA}}/M_{\mathrm{qp}}$ kaikille massaluvuille A, joille laskettiin vähintään kaksi YME:ä.

Aiempiin tutkimuksiin pohjautuen tutkimushypoteesi oli, että tästä saadaan jokin siisti A:n funktio, ehkä jopa vakio. Kuvan 3 perusteella suuri osa pisteistä on lähellä arvoa $k = 0{,}45$, mutta osa k-arvoista on selvästi pienempiä. Kerroin k on matala massaluvuille 60, 108, 110, 136, 138 ja 146. Massaluvuille löydettiin yksi yhteinen tekijä: ainakin yhdessä lasketussa siirtymässä toinen ydin oli puolimaaginen. Tämän havainnon perusteella puolimaagiset ytimet päätettiin käsitellä erikseen.

Artikkelissa [3] $\beta^{\pm}$-YME:ien geometristen keskiarvojen suhde oli vakio A:n funktiona pienellä varianssilla. Vastaavasti tutkittiin, miten geometristen keskiarvojen suhde käyttäytyy korkeasti kiellettyjen siirtymien tapauksessa, kun YME:illä on yhteinen lähtö- tai tytärydin. Tulokset ovat näkyvissä tutkielman kuvassa 4: k ei ole A:n funktiona näkyvästi sileämpi. Niinpä päädyttiin käyttämään kaikkia laskettuja siirtymiä k:n määrittämiseen. Suurin osa näin saaduista suhteista k (tutkielman kuva 3) oli joko noin $5 \cdot 10^{-1}$ tai $2 \cdot 10^{-3}$, joten oli luonnollista jakaa pisteet kahteen ryhmään (GROUP 1 ja 2). Arvo $k = 0{,}01$ osoittautui sopivaksi jakopisteeksi: lähes kaikki k-arvot olivat tätä arvoa joko yhden magnitudin suurempia tai pienempiä.

Koska massaluvun A vaikutuksen lisäksi kielletyn siirtymän kertaluvun K

vaikutusta ei tunnettu, merkittiin siirtymän kertaluku tutkielman kuviin 3 ja 4 värikoodilla.

Koska hyvin pieniä k-arvoja ei ollut aiemmissa tutkimuksissa havaittu, ei ollut itsestäänselvää, oliko kyse virheestä laskuissa vai käytettyjen ydinmallien rajoituksista. Mielenkiintoista oli, että osassa puolimaagisen ytimen sisältävistä siirtymistä siirtymän k-arvo oli korkea. Matalien k-arvojen syyn selvittämiseksi verrattiin siirtymiä $^{114}\mathrm{Sb} \rightarrow {}^{114}\mathrm{Sn}$ ja $^{112}\mathrm{Sb} \rightarrow {}^{112}\mathrm{Sn}$ vastaavien YME:ien käytöstä. Näiden siirtymien YME:ien suhteessa oli kahden magnitudin ero. Vertaamalla protoni–neutroni-konfiguraatioiden kontribuutioita matriisielementtiin huomattiin, että perustilan konfiguraatio on tinaisotoopeilla erilainen. Muuttamalla manuaalisesti protoniorbitaalin $0\mathrm{h}_{11/2}$ energiaa saatiin M_{pnQRPA}:n arvo hyppäämään kaksi magnitudia pisteessä, jossa perustilan johtavien kontribuutioiden konfiguraatiot vaihtuvat. BCS-lasku tuottaa puolimaagiselle ytimelle miehitysluvuiksi lähellä nollaa tai ykköstä olevat luvut, joten muutos aiheuttaa noin 500-kertaisen muutoksen YME:n arvossa. Muiden puolimaagisia ytimiä sisältävien siirtymien pienet k-arvot johtunevat samasta ilmiöstä.

Viitteet

[1] A. Bohr ja B. R. Mottelson, Nuclear Structure, Vol. I, Benjamin, New York, (1969).

[2] H. Ejiri and J. Suhonen, J. Phys. G: Nucl. Part. Phys. 42, 055201 (2015).

[3] H. Ejiri, N. Soukouti, and J. Suhonen, Phys. Lett. B 729, 27 (2014).

[4] N. B. Gove and M. Martin, At. Data and Nucl. Data Tables 10, 205 (1971).

[5] E. Ydrefors, M. T. Mustonen, and J. Suhonen, Nucl. Phys. A 842, 33 (2010).

[6] Taylor, John R. *An Introduction to Error Analysis, Second Edition*, University Science Books Sausalito Ca., 1997

Liitteet

Taulukko 1: Kahdesti kiellettyjen siirtymien matriisielementit ja faasiavaruusintegraalit virheineen.

Siirtymä	Tyyppi	p–n-konf.	$\lvert M_{\mathrm{pnQRPA}}\rvert$ [fm^2]	$\lvert M_{\mathrm{qp}}\rvert$ [fm^2]	f_{2u}
$^{52}\mathrm{Ti} \rightarrow {}^{52}\mathrm{V}$	β^-	$0\mathrm{d}_{3/2} - 0\mathrm{g}_{9/2}$	$1.82(2) \cdot 10^{-4}$	$6.68 \cdot 10^{-4}$	66(2)
$^{52}\mathrm{Sc} \rightarrow {}^{52}\mathrm{Ti}$	β^-	$0\mathrm{d}_{3/2} - 0\mathrm{g}_{9/2}$	$1.82(3) \cdot 10^{-4}$	$6.68 \cdot 10^{-4}$	$1.98(3) \cdot 10^{7}$
$^{54}\mathrm{Mn} \rightarrow {}^{54}\mathrm{Fe}$	β^-	$0\mathrm{d}_{3/2} - 0\mathrm{g}_{9/2}$	$3.43(2) \cdot 10^{-4}$	$6.83 \cdot 10^{-4}$	$3.9(5) \cdot 10^{-2}$
$^{54}\mathrm{Mn} \rightarrow {}^{54}\mathrm{Cr}$	EC	$0\mathrm{g}_{9/2} - 0\mathrm{d}_{3/2}$	$1.77(2) \cdot 10^{-4}$	$6.88 \cdot 10^{-4}$	$8.70(18) \cdot 10^{-2}$
	β^+				$7.29(11) \cdot 10^{-5}$
	EC/β^+				$8.71(11) \cdot 10^{-2}$
$^{56}\mathrm{Cr} \rightarrow {}^{56}\mathrm{Mn}$	β^-	$0\mathrm{d}_{3/2} - 0\mathrm{g}_{9/2}$	$2.80(2) \cdot 10^{-4}$	$6.78 \cdot 10^{-4}$	16(2)
$^{56}\mathrm{Mn} \rightarrow {}^{56}\mathrm{Fe}$	β^-	$0\mathrm{d}_{3/2} - 0\mathrm{g}_{9/2}$	$2.72(2) \cdot 10^{-4}$	$6.87 \cdot 10^{-4}$	$1.01(5) \cdot 10^{4}$
$^{58}\mathrm{Mn}^* \rightarrow {}^{58}\mathrm{Fe}$	β^-	$0\mathrm{d}_{3/2} - 0\mathrm{g}_{9/2}$	$2.98(2) \cdot 10^{-4}$	$6.89 \cdot 10^{-4}$	$1.06(5) \cdot 10^{6}$
$^{58}\mathrm{Co}^* \rightarrow {}^{58}\mathrm{Fe}$	EC	$0\mathrm{g}_{9/2} - 0\mathrm{d}_{3/2}$	$1.66(2) \cdot 10^{-4}$	$7.02 \cdot 10^{-4}$	3.36(10)
	β^+				1.29(8)
	EC/β^+				4.64(18)
$^{94}\mathrm{Nb}^* \rightarrow {}^{94}\mathrm{Mo}$	β^-	$0\mathrm{f}_{5/2} - 0\mathrm{h}_{11/2}$	$2.96(2) \cdot 10^{-4}$	$1.13 \cdot 10^{-3}$	186(12)
$^{94}\mathrm{Nb}^* \rightarrow {}^{94}\mathrm{Zr}$	EC	$0\mathrm{h}_{11/2} - 0\mathrm{f}_{5/2}$	$3.78(3) \cdot 10^{-4}$	$1.18 \cdot 10^{-3}$	$4.5(7) \cdot 10^{-2}$
$^{110}\mathrm{Sb} \rightarrow {}^{110}\mathrm{Sn}$	EC	$0\mathrm{h}_{11/2} - 0\mathrm{f}_{5/2}$	$2.93(12) \cdot 10^{-7}$	$1.23 \cdot 10^{-3}$	$5.78(7) \cdot 10^{4}$
	β^+				$6.1(2) \cdot 10^{5}$
	EC/β^+				$6.7(2) \cdot 10^{5}$
$^{112}\mathrm{Sb} \rightarrow {}^{112}\mathrm{Sn}$	EC	$0\mathrm{h}_{11/2} - 0\mathrm{f}_{5/2}$	$1.53(6) \cdot 10^{-6}$	$1.24 \cdot 10^{-3}$	$2.03(4) \cdot 10^{4}$
	β^+				$1.13(3) \cdot 10^{5}$
	EC/β^+				$1.33(4) \cdot 10^{5}$
$^{114}\mathrm{Te} \rightarrow {}^{114}\mathrm{Sb}$	EC	$0\mathrm{h}_{11/2} - 0\mathrm{f}_{5/2}$	$5.03(4) \cdot 10^{-4}$	$1.24 \cdot 10^{-3}$	53.1(5)
	β^+				2.19(5)
	EC/β^+				55.3(6)
$^{114}\mathrm{Sb} \rightarrow {}^{114}\mathrm{Sn}$	EC	$0\mathrm{h}_{11/2} - 0\mathrm{f}_{5/2}$	$5.77(4) \cdot 10^{-4}$	$1.25 \cdot 10^{-3}$	$8.1(2) \cdot 10^{3}$
	β^+				$2.5(1) \cdot 10^{4}$
	EC/β^+				$3.3(2) \cdot 10^{4}$
$^{116}\mathrm{Te} \rightarrow {}^{116}\mathrm{Sb}$	EC	$0\mathrm{h}_{11/2} - 0\mathrm{f}_{5/2}$	$3.30(3) \cdot 10^{-4}$	$1.25 \cdot 10^{-3}$	2.19(3)
	β^+				$5.9(3) \cdot 10^{-4}$
	EC/β^+				2.19(3)
$^{116}\mathrm{Sb} \rightarrow {}^{116}\mathrm{Sn}$	EC	$0\mathrm{h}_{11/2} - 0\mathrm{f}_{5/2}$	$6.05(4) \cdot 10^{-4}$	$1.25 \cdot 10^{-3}$	$1.75(2) \cdot 10^{3}$
	β^+				$1.85(3) \cdot 10^{3}$
	EC/β^+				$3.61(4) \cdot 10^{3}$
$^{130}\mathrm{Ce} \rightarrow {}^{130}\mathrm{La}$	EC	$0\mathrm{h}_{11/2} - 0\mathrm{f}_{5/2}$	$5.33(4) \cdot 10^{-4}$	$1.24 \cdot 10^{-3}$	28.6(4)
	β^+				$2.00(6) \cdot 10^{-1}$
	EC/β^+				28.8(4)
$^{130}\mathrm{La} \rightarrow {}^{130}\mathrm{Ba}$	EC	$0\mathrm{h}_{11/2} - 0\mathrm{f}_{5/2}$	$5.28(4) \cdot 10^{-4}$	$1.25 \cdot 10^{-3}$	$8.09(3) \cdot 10^{3}$
	β^+				$1.09(6) \cdot 10^{4}$
	EC/β^+				$1.90(9) \cdot 10^{4}$
$^{132}\mathrm{Sn} \rightarrow {}^{132}\mathrm{Sb}^*$	β^-	$0\mathrm{h}_{11/2} - 0\mathrm{f}_{5/2}$	$1.03(1) \cdot 10^{-4}$	$1.31 \cdot 10^{-3}$	$4(3) \cdot 10^{3}$

Taulukko 2: Kolmesti kiellettyjen siirtymien matriisielementit ja faasiavaruusintegraalit virheineen.

Siirtymä	Tyyppi	p–n-konf.	$\lvert M_{\mathrm{pnQRPA}}\rvert$ [fm^3]	$\lvert M_{\mathrm{qp}}\rvert$ [fm^3]	f_{3u}
^{74}Zn $\rightarrow$ ^{74}Ga*	β^-	$0f_{7/2} - 1d_{5/2}$	$4.04(3) \cdot 10^{-6}$	$8.84 \cdot 10^{-6}$	47(4)
^{74}Ga* $\rightarrow$ ^{74}Ge	β^-	$1p_{3/2} - 1d_{5/2}$	$6.30(5) \cdot 10^{-6}$	$1.11 \cdot 10^{-5}$	$4.2(2) \cdot 10^5$
^{74}Kr $\rightarrow$ ^{74}Br*	EC	$1d_{5/2} - 1p_{3/2}$	$7.27(5) \cdot 10^{-6}$	$1.38 \cdot 10^{-5}$	11.3(3)
	β^+				1.12(4)
	EC/β^+				12.5(3)
^{74}Br* $\rightarrow$ ^{74}Se	EC	$1d_{5/2} - 1p_{3/2}$	$4.70(4) \cdot 10^{-6}$	$1.43 \cdot 10^{-5}$	$2.13(2) \cdot 10^4$
	β^+				$3.04(4) \cdot 10^5$
	EC/β^+				$3.26(4) \cdot 10^5$
^{86}Zr $\rightarrow$ ^{86}Y	EC	$1d_{5/2} - 1p_{3/2}$	$6.18(5) \cdot 10^{-6}$	$1.54 \cdot 10^{-5}$	$4.1(5) \cdot 10^{-2}$
	β^+				$1.9(6) \cdot 10^{-7}$
	EC/β^+				$4.1(5) \cdot 10^{-2}$
^{86}Y $\rightarrow$ ^{86}Sr	EC	$1d_{5/2} - 1p_{3/2}$	$9.04(6) \cdot 10^{-6}$	$1.55 \cdot 10^{-5}$	$2.64(6) \cdot 10^3$
	β^+				$6.5(3) \cdot 10^3$
	EC/β^+				$9.2(3) \cdot 10^3$
^{88}Mo $\rightarrow$ ^{88}Nb	EC	$1d_{5/2} - 1p_{3/2}$	$6.04(4) \cdot 10^{-6}$	$1.55 \cdot 10^{-5}$	131(2)
	β^+				30.2(8)
	EC/β^+				162(3)
^{88}Nb $\rightarrow$ ^{88}Zr	EC	$1d_{5/2} - 1p_{3/2}$	$7.38(5) \cdot 10^{-6}$	$1.57 \cdot 10^{-5}$	$5.83(4) \cdot 10^4$
	β^+				$4.58(5) \cdot 10^5$
	EC/β^+				$5.17(5) \cdot 10^5$
^{88}Zr $\rightarrow$ ^{88}Y	EC	$1d_{5/2} - 1p_{3/2}$	$7.38(5) \cdot 10^{-6}$	$1.57 \cdot 10^{-5}$	$1.6(2) \cdot 10^-4$
^{88}Y $\rightarrow$ ^{88}Sr	EC	$0h_{11/2} - 0g_{9/2}$	$9.95(7) \cdot 10^{-6}$	$1.63() \cdot 10^{-5}$	136(5)
	β^+				53(4)
	EC/β^+				189(8)
^{90}Mo $\rightarrow$ ^{90}Nb*	EC	$1d_{5/2} - 1p_{3/2}$	$6.89(5) \cdot 10^{-6}$	$1.58 \cdot 10^{-5}$	5.6(6)
	β^+				$9(2) \cdot 10^{-2}$
	EC/β^+				5.7(6)
^{90}Nb* $\rightarrow$ ^{90}Zr	EC	$0h_{11/2} - 0g_{9/2}$	$8.60(6) \cdot 10^{-6}$	$1.65 \cdot 10^{-5}$	$1.28(5) \cdot 10^4$
	β^+				$5.5(3) \cdot 10^4$
	EC/β^+				$6.7(4) \cdot 10^4$
^{146}Gd $\rightarrow$ ^{146}Eu	EC	$1d_{3/2} - 0h_{11/2}$	$6.34(25) \cdot 10^{-8}$	$2.54 \cdot 10^{-5}$	$2.8(2) \cdot 10^{-2}$
	β^+				$9.8(9) \cdot 10^{-17}$
	EC/β^+				$2.8(2) \cdot 10^{-2}$
^{146}Eu $\rightarrow$ ^{146}Sm	EC	$1d_{3/2} - 0h_{11/2}$	$7.32(5) \cdot 10^{-6}$	$2.57 \cdot 10^{-5}$	$1.46(2) \cdot 10^3$
	β^+				92(2)
	EC/β^+				$1.55(3) \cdot 10^3$

Taulukko 3: Neljästi kiellettyjen siirtymien matriisielementit ja faasiavaruusintegraalit virheineen.

Siirtymä	Tyyppi	p–n-konf.	$\lvert M_{\mathrm{pnQRPA}}\rvert$ [fm^4]	$\lvert M_{\mathrm{qp}}\rvert$ [fm^4]	f_{4u}
$^{50}\mathrm{Sc} \to {}^{50}\mathrm{Ti}$	β^-	$1\mathrm{s}_{1/2} - 0\mathrm{g}_{9/2}$	$7.55(5) \cdot 10^{-8}$	$1.48 \cdot 10^{-7}$	$5.7(2) \cdot 10^{6}$
$^{60}\mathrm{Fe} \to {}^{60}\mathrm{Co}$	β^-	$1\mathrm{s}_{1/2} - 0\mathrm{g}_{9/2}$	$7.23(5) \cdot 10^{-8}$	$1.62 \cdot 10^{-7}$	$2.7(4) \cdot 10^{-9}$
$^{60}\mathrm{Co} \to {}^{60}\mathrm{Ni}$	β^-	$1\mathrm{s}_{1/2} - 0\mathrm{g}_{9/2}$	$5.30(3) \cdot 10^{-10}$	$1.64 \cdot 10^{-7}$	17(2)
$^{98}\mathrm{Pd} \to {}^{98}\mathrm{Rh}$	EC	$0\mathrm{h}_{11/2} - 1\mathrm{p}_{1/2}$	$6.55(5) \cdot 10^{-8}$	$3.21 \cdot 10^{-7}$	$1.7(2) \cdot 10^{-1}$
	β^+				$4.4(8) \cdot 10^{-5}$
	EC/β^+				$1.7(2) \cdot 10^{-1}$
$^{98}\mathrm{Rh} \to {}^{98}\mathrm{Ru}$	EC	$0\mathrm{h}_{11/2} - 1\mathrm{p}_{1/2}$	$1.20(1) \cdot 10^{-7}$	$3.20 \cdot 10^{-7}$	$3.94(8) \cdot 10^{3}$
	β^+				$2.08(7) \cdot 10^{3}$
	EC/β^+				$6.0(2) \cdot 10^{3}$
$^{102}\mathrm{Cd} \to {}^{102}\mathrm{Ag}$	EC	$0\mathrm{h}_{11/2} - 1\mathrm{p}_{1/2}$	$6.40(5) \cdot 10^{-8}$	$3.28 \cdot 10^{-7}$	5.9(2)
	β^+				$3.7(3) \cdot 10^{-2}$
	EC/β^+				5.9(2)
$^{102}\mathrm{Ag} \to {}^{102}\mathrm{Pd}$	EC	$1\mathrm{d}_{5/2} - 1\mathrm{d}_{5/2}$	$1.16(1) \cdot 10^{-7}$	$3.48 \cdot 10^{-7}$	$1.52(3) \cdot 10^{4}$
	β^+				$1.16(3) \cdot 10^{4}$
	EC/β^+				$2.67(6) \cdot 10^{4}$
$^{104}\mathrm{Cd} \to {}^{104}\mathrm{Ag}$	EC	$1\mathrm{d}_{5/2} - 1\mathrm{d}_{5/2}$	$7.68(5) \cdot 10^{-8}$	$3.47 \cdot 10^{-7}$	$1.48(7) \cdot 10^{-3}$
	β^+				$8(4) \cdot 10^{-13}$
	EC/β^+				$1.48(7) \cdot 10^{-3}$
$^{104}\mathrm{Ag} \to {}^{104}\mathrm{Pd}$	EC	$1\mathrm{d}_{5/2} - 1\mathrm{d}_{5/2}$	$1.40(1) \cdot 10^{-7}$	$3.79 \cdot 10^{-7}$	872(9)
	β^+				163(3)
	EC/β^+				$1.04(2) \cdot 10^{4}$
$^{130}\mathrm{I} \to {}^{130}\mathrm{Te}$	EC	$1\mathrm{d}_{5/2} - 1\mathrm{d}_{5/2}$	$2.45(2) \cdot 10^{-8}$	$4.85 \cdot 10^{-7}$	$4.3(4) \cdot 10^{-8}$
$^{130}\mathrm{I} \to {}^{130}\mathrm{Xe}$	β^-	$1\mathrm{p}_{3/2} - 1\mathrm{f}_{7/2}$	$4.60(3) \cdot 10^{-9}$	$3.96 \cdot 10^{-7}$	630(8)
$^{136}\mathrm{Cs} \to {}^{136}\mathrm{Xe}$	EC	$1\mathrm{d}_{5/2} - 1\mathrm{d}_{5/2}$	$1.39(6) \cdot 10^{-9}$	$4.81 \cdot 10^{-7}$	$5(1\ \mathrm{mag}) \cdot 10^{-17}$
$^{136}\mathrm{Cs} \to {}^{136}\mathrm{Ba}$	β^-	$1\mathrm{p}_{3/2} - 1\mathrm{f}_{7/2}$	$3.40(2) \cdot 10^{-9}$	$4.07 \cdot 10^{-7}$	131(12)
$^{138}\mathrm{La} \to {}^{138}\mathrm{Ba}$	EC	$0\mathrm{h}_{11/2} - 0\mathrm{h}_{11/2}$	$1.09(13) \cdot 10^{-9}$	$4.68 \cdot 10^{-7}$	$1.91(4) \cdot 10^{-1}$
	β^+				$7.8(4) \cdot 10^{-6}$
	EC/β^+		$1.91(4) \cdot 10^{-1}$		
$^{138}\mathrm{La} \to {}^{138}\mathrm{Ce}$	β^-	$1\mathrm{p}_{1/2} - 1\mathrm{f}_{7/2}$	$4.41(3) \cdot 10^{-9}$	$4.10 \cdot 10^{-7}$	$1.0(1) \cdot 10^{-2}$

Taulukko 4: Kuudesti kiellettyjen siirtymien matriisielementit ja faasiavaruusintegraalit virheineen.

Siirtymä	Tyyppi	p–n-konf.	$\lvert M_{\mathrm{pnQRPA}}\rvert$ [fm^6]	$\lvert M_{\mathrm{qp}}\rvert$ [fm^6]	f_{6u}
$^{92}\mathrm{Nb} \rightarrow {}^{92}\mathrm{Zr}$	EC	$1\mathrm{d}_{5/2} - 0\mathrm{g}_{9/2}$	$6.96(5) \cdot 10^{-11}$	$1.57 \cdot 10^{-10}$	$9(2) \cdot 10^{-3}$
	β^+				$2.9(11) \cdot 10^{-7}$
	EC/β^+				$9(2) \cdot 10^{-3}$
$^{92}\mathrm{Nb} \rightarrow {}^{92}\mathrm{Mo}$	β^-	$1\mathrm{p}_{3/2} - 0\mathrm{h}_{11/2}$	$8.53(6) \cdot 10^{-11}$	$1.43 \cdot 10^{-10}$	$1(1\ \mathrm{mag}) \cdot 10^{-11}$
$^{94}\mathrm{Ru} \rightarrow {}^{94}\mathrm{Tc}$	EC	$1\mathrm{d}_{5/2} - 0\mathrm{g}_{9/2}$	$5.20(2) \cdot 10^{-13}$	$1.61 \cdot 10^{-10}$	$3.7(2) \cdot 10^{-4}$
	β^+				$2.1(3) \cdot 10^{-10}$
	EC/β^+				$3.7(2) \cdot 10^{-4}$
$^{94}\mathrm{Tc} \rightarrow {}^{94}\mathrm{Mo}$	EC	$1\mathrm{d}_{5/2} - 0\mathrm{g}_{9/2}$	$6.03(4) \cdot 10^{-11}$	$1.59 \cdot 10^{-10}$	442(6)
	β^+				10.9(3)
	EC/β^+				453(7)
$^{96}\mathrm{Tc} \rightarrow {}^{96}\mathrm{Mo}$	EC	$1\mathrm{d}_{5/2} - 0\mathrm{g}_{9/2}$	$8.47(6) \cdot 10^{-11}$	$1.62 \cdot 10^{-10}$	2.81(7)
	β^+				$5.6(3) \cdot 10^{-3}$
	EC/β^+				2.81(7)
$^{96}\mathrm{Tc} \rightarrow {}^{96}\mathrm{Ru}$	β^-	$1\mathrm{p}_{3/2} - 0\mathrm{h}_{11/2}$	$8.88(6) \cdot 10^{-11}$	$1.49 \cdot 10^{-10}$	$4(2) \cdot 10^{-13}$
$^{108}\mathrm{Sn} \rightarrow {}^{108}\mathrm{In}$	EC	$1\mathrm{d}_{5/2} - 0\mathrm{g}_{9/2}$	$2.52(10) \cdot 10^{-13}$	$1.79 \cdot 10^{-10}$	$2.4(2) \cdot 10^{-2}$
	β^+				$5.9(9) \cdot 10^{-7}$
	EC/β^+				$2.4(2) \cdot 10^{-2}$
$^{108}\mathrm{In} \rightarrow {}^{108}\mathrm{Cd}$	EC	$1\mathrm{d}_{5/2} - 0\mathrm{g}_{9/2}$	$6.05(4) \cdot 10^{-11}$	$1.79 \cdot 10^{-10}$	$1.0(3) \cdot 10^{3}$
	β^+				403(14)
	EC/β^+				$1.0(3) \cdot 10^{4}$
$^{110}\mathrm{Sn} \rightarrow {}^{110}\mathrm{In}$	EC	$1\mathrm{d}_{5/2} - 0\mathrm{g}_{9/2}$	$2.55(10) \cdot 10^{-13}$	$1.82 \cdot 10^{-10}$	$9(6) \cdot 10^{-10}$
$^{110}\mathrm{In} \rightarrow {}^{110}\mathrm{Cd}$	EC	$1\mathrm{d}_{5/2} - 0\mathrm{g}_{9/2}$	$6.45(5) \cdot 10^{-11}$	$1.82 \cdot 10^{-10}$	191(9)
	β^+				1.5(1)
	EC/β^+				192(9)

Taulukko 5: Seitsemästi kiellettyjen siirtymien matriisielementit ja faasiavaruusintegraalit virheineen.

Siirtymä	Tyyppi	p–n-konf.	$\lvert M_{\mathrm{pnQRPA}}\rvert$ [fm^7]	$\lvert M_{\mathrm{qp}}\rvert$ [fm^7]	f_{7u}
$^{126}\mathrm{Sn} \rightarrow {}^{126}\mathrm{Sb}$	β^-	$0\mathrm{g}_{9/2} - 1\mathrm{f}_{7/2}$	$6.12(24) \cdot 10^{-15}$	$5.53 \cdot 10^{-12}$	$1.71(3) \cdot 10^{4}$
$^{132}\mathrm{Sn} \rightarrow {}^{132}\mathrm{Sb}$	β^-	$0\mathrm{g}_{9/2} - 1\mathrm{f}_{7/2}$	$8.66(33) \cdot 10^{-18}$	$5.84 \cdot 10^{-12}$	493(12)

Taulukko 6: Puoliintumisajat kahdesti kielletyille siirtymille. "Kokeellisten" arvojen (oikeanpuoleisin sarake) virheissä on otettu huomioon kertoimen k_{NM} epätarkkuus.

Siirtymä	Tyyppi	p–n-konf.	$t_{1/2}$(pnQRPA)	$t_{1/2}$(qp)	Arvioitu $t_{1/2}$
$^{52}\mathrm{Ti} \rightarrow {}^{52}\mathrm{V}$	β^-	$0\mathrm{d}_{3/2} - 0\mathrm{g}_{9/2}$	57(2) a	4.3(2) a	130(30) a
$^{52}\mathrm{Sc} \rightarrow {}^{52}\mathrm{Ti}$	β^-	$0\mathrm{d}_{3/2} - 0\mathrm{g}_{9/2}$	9.9(2) h	52(1) min	22(5) h
$^{54}\mathrm{Mn} \rightarrow {}^{54}\mathrm{Fe}$	β^-	$0\mathrm{d}_{3/2} - 0\mathrm{g}_{9/2}$	$1.9(3) \cdot 10^5$ a	$4.8(6) \cdot 10^4$ a	$9(3) \cdot 10^5$ a
$^{54}\mathrm{Mn} \rightarrow {}^{54}\mathrm{Cr}$	EC	$0\mathrm{g}_{9/2} - 0\mathrm{d}_{3/2}$	$3.2(7) \cdot 10^5$ a	$2.1(4) \cdot 10^4$ a	$7(2) \cdot 10^5$ a
	β^+		$3.8(7) \cdot 10^8$ a	$2.5(7) \cdot 10^7$ a	$9(2) \cdot 10^8$ a
	EC/β^+		$3.2(7) \cdot 10^5$ a	$2.1(6) \cdot 10^4$ a	$7(2) \cdot 10^5$ a
$^{56}\mathrm{Cr} \rightarrow {}^{56}\mathrm{Mn}$	β^-	$0\mathrm{d}_{3/2} - 0\mathrm{g}_{9/2}$	97.6(9) a	35(4) a	210(50) a
$^{56}\mathrm{Mn} \rightarrow {}^{56}\mathrm{Fe}$	β^-	$0\mathrm{d}_{3/2} - 0\mathrm{g}_{9/2}$	1.17(6) a	67(4) d	2.6(6) a
$^{58}\mathrm{Mn}^* \rightarrow {}^{58}\mathrm{Fe}$	β^-	$0\mathrm{d}_{3/2} - 0\mathrm{g}_{9/2}$	3.39(5) d	15.2(2) h	8(2) d
$^{58}\mathrm{Co}^* \rightarrow {}^{58}\mathrm{Fe}$	EC	$0\mathrm{g}_{9/2} - 0\mathrm{d}_{3/2}$	$9.5(3) \cdot 10^3$ a	530(20) a	$2.1(5) \cdot 10^4$ a
	β^+		2.5(2) a	$1.38(9) \cdot 10^3$ a	6(2) a
	EC/β^+		6.9(3) a	380(20) a	15(4) a
$^{94}\mathrm{Nb}^* \rightarrow {}^{94}\mathrm{Mo}$	β^-	$0\mathrm{f}_{5/2} - 0\mathrm{h}_{11/2}$	54(4) a	3.7(3) a	120(30) a
$^{94}\mathrm{Nb}^* \rightarrow {}^{94}\mathrm{Zr}$	EC	$0\mathrm{h}_{11/2} - 0\mathrm{f}_{5/2}$	$1.4(3) \cdot 10^5$ a	$1.4(3) \cdot 10^4$ a	$3(8) \cdot 10^5$ a
$^{110}\mathrm{Sb} \rightarrow {}^{110}\mathrm{Sn}$	EC	$0\mathrm{h}_{11/2} - 0\mathrm{f}_{5/2}$	$1.8(2) \cdot 10^5$ a	3.6(3) d	$5(1) \cdot 10^5$ a
	β^+		$1.7(2) \cdot 10^4$ a	8.3(7) h	$9(2) \cdot 10^4$ a
	EC/β^+		$1.5(2) \cdot 10^4$ a	7.6(6) h	$7(2) \cdot 10^4$ a
$^{112}\mathrm{Sb} \rightarrow {}^{112}\mathrm{Sn}$	EC	$0\mathrm{h}_{11/2} - 0\mathrm{f}_{5/2}$	$1.8(2) \cdot 10^4$ a	10.2(8) d	$9(2) \cdot 10^4$ a
	β^+		$3.3(3) \cdot 10^3$ a	1.9(2) d	$1.6(4) \cdot 10^4$ a
	EC/β^+		$2.8(3) \cdot 10^3$ a	1.6(2) d	$1.4(4) \cdot 10^4$ a
$^{114}\mathrm{Te} \rightarrow {}^{114}\mathrm{Sb}$	EC	$0\mathrm{h}_{11/2} - 0\mathrm{f}_{5/2}$	9.3(2) a	1.54(3) a	44(9) a
	β^+		255(6) a	37.3(9) a	$1.2(3) \cdot 10^3$ a
	EC/β^+		8.9(2) a	1.48(3) a	42(9) a
$^{114}\mathrm{Sb} \rightarrow {}^{114}\mathrm{Sn}$	EC	$0\mathrm{h}_{11/2} - 0\mathrm{f}_{5/2}$	118(4) d	25.3(7) d	2.4(5) a
	β^+		39(2) d	8.3(4) d	180(40) d
	EC/β^+		29(2) d	6.2(3) d	140(30) d
$^{116}\mathrm{Te} \rightarrow {}^{116}\mathrm{Sb}$	EC	$0\mathrm{h}_{11/2} - 0\mathrm{f}_{5/2}$	521(9) a	36.5(7) a	$2.5(5) \cdot 10^3$ a
	β^+		$1.94(9) \cdot 10^6$ a	$1.36(6) \cdot 10^5$ a	$9(2) \cdot 10^6$ a
	EC/β^+		521(9) a	36.5(7) a	$2.5(5) \cdot 10^3$ a
$^{116}\mathrm{Sb} \rightarrow {}^{116}\mathrm{Sn}$	EC	$0\mathrm{h}_{11/2} - 0\mathrm{f}_{5/2}$	1.36(2) a	166(2) d	6(2) a
	β^+		1.29(3) a	110(2) d	6(2) a
	EC/β^+		241(4) d	56.4(9) d	3.1(7) a
$^{130}\mathrm{Ce} \rightarrow {}^{130}\mathrm{La}$	EC	$0\mathrm{h}_{11/2} - 0\mathrm{f}_{5/2}$	15.4(3) a	2.85(5) a	70(20) a
	β^+		410(70) a	2.85(2) a	$1.9(4) \cdot 10^3$ a
	EC/β^+		15.2(3) a	2.83(5) a	70(20) a
$^{130}\mathrm{La} \rightarrow {}^{130}\mathrm{Ba}$	EC	$0\mathrm{h}_{11/2} - 0\mathrm{f}_{5/2}$	141(2) d	25.0(4) d	1.8(4) a
	β^+		105(2) d	18.6(3) d	1.4(3) a
	EC/β^+		60(1) d	10.7(2) d	280(60) d
$^{132}\mathrm{Sn} \rightarrow {}^{132}\mathrm{Sb}^*$	β^-	$0\mathrm{h}_{11/2} - 0\mathrm{f}_{5/2}$	3(2) a	30(20) d	10(7) a

Taulukko 7: Sama kuin taulukko 6 kolmesti kielletyille siirtymille.

Siirtymä	Tyyppi	p–n-konf.	$t_{1/2}$(pnQRPA)	$t_{1/2}$(qp)	Arvioitu $t_{1/2}$
^{74}Zn $\rightarrow$ ^{74}Ga*	β^{-}	$0f_{7/2} - 1d_{5/2}$	$1.6(1) \cdot 10^{5}$ a	$3.4(2) \cdot 10^{3}$ a	$3.5(8) \cdot 10^{5}$ a
^{74}Ga* $\rightarrow$ ^{74}Ge	β^{-}	$1p_{3/2} - 1d_{5/2}$	68(3) a	21.7(7) a	150(40) a
^{74}Kr $\rightarrow$ ^{74}Br*	EC	$1d_{5/2} - 1p_{3/2}$	$2.08(5) \cdot 10^{5}$ a	$5.8(2) \cdot 10^{4}$ a	$5(1) \cdot 10^{5}$ a
	β^{+}		$2.11(8) \cdot 10^{6}$ a	$5.9(2) \cdot 10^{5}$ a	$5(1) \cdot 10^{6}$ a
	EC/β^{+}		$1.90(5) \cdot 10^{5}$ a	$5.3(2) \cdot 10^{4}$ a	$4.2(9) \cdot 10^{5}$ a
^{74}Br* $\rightarrow$ ^{74}Se	EC	$1d_{5/2} - 1p_{3/2}$	2.39(4) a	259(4) a	5(2) a
	β^{+}		167(3) a	18.1(3) a	370(80) a
	EC/β^{+}		156(3) a	16.9(3) a	340(70) a
^{86}Zr $\rightarrow$ ^{86}Y	EC	$1d_{5/2} - 1p_{3/2}$	$7.9(8) \cdot 10^{7}$ a	$1.3(2) \cdot 10^{7}$ a	$1.7(4) \cdot 10^{8}$ a
	β^{+}		$1.7(9) \cdot 10^{13}$ a	$3(2) \cdot 10^{12}$ a	$3(2) \cdot 10^{13}$ a
	EC/β^{+}		$7.9(8) \cdot 10^{7}$ a	$1.3(2) \cdot 10^{7}$ a	$1.8(5) \cdot 10^{8}$ a
^{86}Y $\rightarrow$ ^{86}Sr	EC	$1d_{5/2} - 1p_{3/2}$	$5.2(2) \cdot 10^{3}$ a	$1.77(5) \cdot 10^{3}$ a	$1.1(3) \cdot 10^{4}$ a
	β^{+}		$2.11(8) \cdot 10^{3}$ a	720(30) a	$5(2) \cdot 10^{3}$ a
	EC/β^{+}		$1.50(5) \cdot 10^{3}$ a	510(20) a	$3.3(7) \cdot 10^{3}$ a
^{88}Mo $\rightarrow$ ^{88}Nb	EC	$1d_{5/2} - 1p_{3/2}$	$2.60(5) \cdot 10^{4}$ a	$3.93(8) \cdot 10^{3}$ a	$6(2) \cdot 10^{4}$ a
	β^{+}		$1.13(3) \cdot 10^{5}$ a	$17.1(5) \cdot 10^{3}$ a	$2.5(6) \cdot 10^{5}$ a
	EC/β^{+}		$2.12(5) \cdot 10^{4}$ a	$3.20(7) \cdot 10^{3}$ a	$5(1) \cdot 10^{4}$ a
^{88}Nb $\rightarrow$ ^{88}Zr	EC	$1d_{5/2} - 1p_{3/2}$	39.3(6) a	8.7(2) a	90(20) a
	β^{+}		5.00(8) a	1.11(2) a	11(3) a
	EC/β^{+}		4.44(8) a	359(6) d	9(2) a
^{88}Zr $\rightarrow$ ^{88}Y	EC	$1d_{5/2} - 1p_{3/2}$	$1.4(1) \cdot 10^{10}$ a	$3.1(3) \cdot 10^{9}$ a	$2.8(7) \cdot 10^{10}$ a
^{88}Y $\rightarrow$ ^{88}Sr	EC	$0h_{11/2} - 0g_{9/2}$	$8.4(3) \cdot 10^{4}$ a	$3.1(1) \cdot 10^{4}$ a	$1.8(4) \cdot 10^{5}$ a
	β^{+}		$2.1(2) \cdot 10^{5}$ a	$7.9(5) \cdot 10^{4}$ a	$5(1) \cdot 10^{5}$ a
	EC/β^{+}		$6.0(3) \cdot 10^{4}$ a	$2.2(1) \cdot 10^{4}$ a	$1.3(3) \cdot 10^{5}$ a
^{90}Mo $\rightarrow$ ^{90}Nb*	EC	$1d_{5/2} - 1p_{3/2}$	$4.7(5) \cdot 10^{5}$ a	$8.9(9) \cdot 10^{4}$ a	$1.0(3) \cdot 10^{6}$ a
	β^{+}		$2.9(6) \cdot 10^{7}$ a	$6(1) \cdot 10^{6}$ a	$6(2) \cdot 10^{7}$ a
	EC/β^{+}		$4.6(5) \cdot 10^{5}$ a	$8.7(8) \cdot 10^{4}$ a	$1.0(3) \cdot 10^{6}$ a
^{90}Nb* $\rightarrow$ ^{90}Zr	EC	$0h_{11/2} - 0g_{9/2}$	131(5) a	36(2) a	290(60) a
	β^{+}		31(2) a	8.4(5) a	70(20) a
	EC/β^{+}		25(2) a	6.8(4) a	60(20) a
^{146}Gd $\rightarrow$ ^{146}Eu	EC	$1d_{3/2} - 0h_{11/2}$	$1.1(1) \cdot 10^{12}$ a	$7.0(7) \cdot 10^{6}$ a	$1.6(4) \cdot 10^{12}$ a
	β^{+}		$3.2(3) \cdot 10^{26}$ a	$2.2(2) \cdot 10^{21}$ a	$3.2(7) \cdot 10^{26}$ a
	EC/β^{+}		$1.1(1) \cdot 10^{12}$ a	$7.0(7) \cdot 10^{6}$ a	$1.1(3) \cdot 10^{12}$ a
^{146}Eu $\rightarrow$ ^{146}Sm	EC	$1d_{3/2} - 0h_{11/2}$	$1.44(3) \cdot 10^{4}$ a	$1.16(2) \cdot 10^{3}$ a	$2.2(5) \cdot 10^{4}$ a
	β^{+}		$2.28(6) \cdot 10^{5}$ a	$18.4(5) \cdot 10^{3}$ a	$3.4(7) \cdot 10^{5}$ a
	EC/β^{+}		$1.35(3) \cdot 10^{4}$ a	$1.1(5) \cdot 10^{3}$ a	$2.0(2) \cdot 10^{4}$ a

Taulukko 8: Sama kuin taulukko 6 neljästi kielletyille siirtymille.

Siirtymä	Tyyppi	p–n-konf.	$t_{1/2}$(pnQRPA)	$t_{1/2}$(qp)	Arvioitu $t_{1/2}$
^{50}Sc $\rightarrow$ ^{50}Ti	β^-	$1s_{1/2} - 0g_{9/2}$	$4.2(2) \cdot 10^4$ a	$1.01(4) \cdot 10^4$ a	$9(2) \cdot 10^4$ a
^{60}Fe $\rightarrow$ ^{60}Co	β^-	$1s_{1/2} - 0g_{9/2}$	$9(1) \cdot 10^{18}$ a	$1.8(2) \cdot 10^{18}$ a	$2.0(5) \cdot 10^{19}$ a
^{60}Co $\rightarrow$ ^{60}Ni	β^-	$1s_{1/2} - 0g_{9/2}$	$2.9(4) \cdot 10^{13}$ a	$3.0(5) \cdot 10^8$ a	$6(2) \cdot 10^{13}$ a
^{98}Pd $\rightarrow$ ^{98}Rh	EC	$0h_{11/2} - 1p_{1/2}$	$1.6(2) \cdot 10^{11}$ a	$7.1(6) \cdot 10^9$ a	$8(2) \cdot 10^{11}$ a
	β^+		$6(1) \cdot 10^{14}$ a	$2.7(5) \cdot 10^{13}$ a	$2.8(8) \cdot 10^{15}$ a
	EC/β^+		$1.6(2) \cdot 10^{11}$ a	$7.1(6) \cdot 10^9$ a	$8(2) \cdot 10^{11}$ a
^{98}Rh $\rightarrow$ ^{98}Ru	EC	$0h_{11/2} - 1p_{1/2}$	$2.40(6) \cdot 10^7$ a	$3.40(8) \cdot 10^6$ a	$1.1(3) \cdot 10^8$ a
	β^+		$4.5(2) \cdot 10^7$ a	$6.4(2) \cdot 10^6$ a	$2.1(5) \cdot 10^8$ a
	EC/β^+		$1.57(5) \cdot 10^7$ a	$2.22(6) \cdot 10^6$ a	$7(2) \cdot 10^7$ a
^{102}Cd $\rightarrow$ ^{102}Ag	EC	$0h_{11/2} - 1p_{1/2}$	$5.2(2) \cdot 10^9$ a	$2.0(7) \cdot 10^8$ a	$2.4(5) \cdot 10^{10}$ a
	β^+		$8.1(5) \cdot 10^{11}$ a	$3.1(2) \cdot 10^{10}$ a	$3.8(8) \cdot 10^{12}$ a
	EC/β^+		$5.2(2) \cdot 10^9$ a	$2.0(7) \cdot 10^8$ a	$2.4(5) \cdot 10^{10}$ a
^{102}Ag $\rightarrow$ ^{102}Pd	EC	$1d_{5/2} - 1d_{5/2}$	$6.8(2) \cdot 10^6$ a	$7.5(2) \cdot 10^5$ a	$3.2(7) \cdot 10^7$ a
	β^+		$8.9(3) \cdot 10^6$ a	$9.8(3) \cdot 10^5$ a	$4.2(9) \cdot 10^7$ a
	EC/β^+		$3.84(9) \cdot 10^6$ a	$4.2(1) \cdot 10^5$ a	$1.8(4) \cdot 10^7$ a
^{104}Cd $\rightarrow$ ^{104}Ag	EC	$1d_{5/2} - 1d_{5/2}$	$1.43(7) \cdot 10^{13}$ a	$7.0(3) \cdot 10^{11}$ a	$7(2) \cdot 10^{13}$ a
	β^+		$3(2) \cdot 10^{22}$ a	$1.3(7) \cdot 10^{21}$ a	$1.4(7) \cdot 10^{23}$ a
	EC/β^+		$1.43(7) \cdot 10^{13}$ a	$7.0(4) \cdot 10^{11}$ a	$7(2) \cdot 10^{13}$ a
^{104}Ag $\rightarrow$ ^{104}Pd	EC	$1d_{5/2} - 1d_{5/2}$	$8.0(2) \cdot 10^7$ a	$1.76(3) \cdot 10^7$ a	$3.8(8) \cdot 10^8$ a
	β^+		$4.28(9) \cdot 10^8$ a	$9.4(2) \cdot 10^7$ a	$2.0(5) \cdot 10^9$ a
	EC/β^+		$6.8(2) \cdot 10^7$ a	$1.48(3) \cdot 10^7$ a	$3.2(7) \cdot 10^8$ a
^{130}I $\rightarrow$ ^{130}Te	EC	$1d_{5/2} - 1d_{5/2}$	$5.3(5) \cdot 10^{19}$ a	$1.4(2) \cdot 10^{17}$ a	$2.5(6) \cdot 10^{20}$ a
^{130}I $\rightarrow$ ^{130}Xe	β^-	$1p_{3/2} - 1f_{7/2}$	$1.03(2) \cdot 10^{11}$ a	$1.39(3) \cdot 10^7$ a	$5(1) \cdot 10^{11}$ a
^{136}Cs $\rightarrow$ ^{136}Xe	EC	$1d_{5/2} - 1d_{5/2}$	$1(2\text{ mag}) \cdot 10^{31}$ a	$1.1(2\text{ mag}) \cdot 10^{26}$ a	$5(2\text{ mag}) \cdot 10^{31}$ a
^{136}Cs $\rightarrow$ ^{136}Ba	β^-	$1p_{3/2} - 1f_{7/2}$	$9.1(8) \cdot 10^{11}$ a	$6.4(6) \cdot 10^7$ a	$4(1) \cdot 10^{12}$ a
^{138}La $\rightarrow$ ^{138}Ba	EC	$0h_{11/2} - 0h_{11/2}$	$6.0(2) \cdot 10^{15}$ a	$3.28(8) \cdot 10^{10}$ a	$9(2) \cdot 10^{15}$ a
	β^+		$1.47(7) \cdot 10^{20}$ a	$8.0(2) \cdot 10^{14}$ a	$2.2(5) \cdot 10^{20}$ a
	EC/β^+		$6.0(2) \cdot 10^{15}$ a	$3.28(8) \cdot 10^{10}$ a	$9(2) \cdot 10^{15}$ a
^{138}La $\rightarrow$ ^{138}Ce	β^-	$1p_{1/2} - 1f_{7/2}$	$7.4(8) \cdot 10^{15}$ a	$8.5(9) \cdot 10^{11}$ a	$1.1(3) \cdot 10^{16}$ a

Taulukko 9: Sama kuin taulukko 6 kuudesti kielletyille siirtymille.

Siirtymä	Tyyppi	p–n-konf.	$t_{1/2}$(pnQRPA)	$t_{1/2}$(qp)	Arvioitu $t_{1/2}$
^{92}Nb $\rightarrow$ ^{92}Zr	EC	$1d_{5/2} - 0g_{9/2}$	$4.2(6) \cdot 10^{19}$ a	$8(2) \cdot 10^{18}$ a	$9(3) \cdot 10^{19}$ a
	β^+		$1.0(3) \cdot 10^{24}$ a	$2.0(6) \cdot 10^{23}$ a	$2.2(8) \cdot 10^{24}$ a
	EC/β^+		$4.2(6) \cdot 10^{19}$ a	$8.4(2) \cdot 10^{18}$ a	$9(3) \cdot 10^{19}$ a
^{92}Nb $\rightarrow$ ^{92}Mo	β^-	$1p_{3/2} - 0h_{11/2}$	$2(1\text{ mag}) \cdot 10^{28}$ a	$7(1\text{ mag}) \cdot 10^{27}$ a	$4(1\text{ mag}) \cdot 10^{28}$ a
^{94}Ru $\rightarrow$ ^{94}Tc	EC	$1d_{5/2} - 0g_{9/2}$	$1.25(1) \cdot 10^{25}$ a	$1.3(2) \cdot 10^{19}$ a	$2.8(7) \cdot 10^{25}$ a
	β^+		$2.20(4) \cdot 10^{31}$ a	$2.3(4) \cdot 10^{25}$ a	$5(2) \cdot 10^{31}$ a
	EC/β^+		$1.25(1) \cdot 10^{25}$ a	$1.3(2) \cdot 10^{19}$ a	$2.8(7) \cdot 10^{25}$ a
^{94}Tc $\rightarrow$ ^{94}Mo	EC	$1d_{5/2} - 0g_{9/2}$	$1.16(3) \cdot 10^{15}$ a	$1.67(3) \cdot 10^{14}$ a	$2.6(6) \cdot 10^{15}$ a
	β^+		$4.7(1) \cdot 10^{16}$ a	$6.7(2) \cdot 10^{15}$ a	$1.0(3) \cdot 10^{17}$ a
	EC/β^+		$1.14(3) \cdot 10^{15}$ a	$1.63(4) \cdot 10^{14}$ a	$2.5(6) \cdot 10^{15}$ a
^{96}Tc $\rightarrow$ ^{96}Mo	EC	$1d_{5/2} - 0g_{9/2}$	$9.3(3) \cdot 10^{16}$ a	$2.55(7) \cdot 10^{16}$ a	$2.0(5) \cdot 10^{17}$ a
	β^+		$4.7(2) \cdot 10^{19}$ a	$1.27(6) \cdot 10^{19}$ a	$1.0(3) \cdot 10^{20}$ a
	EC/β^+		$5.3(3) \cdot 10^{16}$ a	$2.55(7) \cdot 10^{16}$ a	$1.2(3) \cdot 10^{17}$ a
^{96}Tc $\rightarrow$ ^{96}Ru	β^-	$1p_{3/2} - 0h_{11/2}$	$5.4(2) \cdot 10^{29}$ a	$1.9(5) \cdot 10^{29}$ a	$1.2(4) \cdot 10^{30}$ a
^{108}Sn $\rightarrow$ ^{108}In	EC	$1d_{5/2} - 0g_{9/2}$	$8.1(9) \cdot 10^{22}$ a	$1.6(2) \cdot 10^{17}$ a	$3.8(9) \cdot 10^{23}$ a
	β^+		$3.3(6) \cdot 10^{27}$ a	$6(1) \cdot 10^{21}$ a	$1.6(5) \cdot 10^{28}$ a
	EC/β^+		$8.1(9) \cdot 10^{22}$ a	$1.6(2) \cdot 10^{17}$ a	$3.8(9) \cdot 10^{23}$ a
^{108}In $\rightarrow$ ^{108}Cd	EC	$1d_{5/2} - 0g_{9/2}$	$5.1(2) \cdot 10^{13}$ a	$5.9(2) \cdot 10^{12}$ a	$2.4(5) \cdot 10^{14}$ a
	β^+		$1.27(5) \cdot 10^{15}$ a	$1.45(6) \cdot 10^{14}$ a	$6(2) \cdot 10^{15}$ a
	EC/β^+		$4.9(2) \cdot 10^{13}$ a	$5.7(2) \cdot 10^{12}$ a	$2.3(5) \cdot 10^{14}$ a
^{110}Sn $\rightarrow$ ^{110}In	EC	$1d_{5/2} - 0g_{9/2}$	$2(1) \cdot 10^{30}$ a	$4(2) \cdot 10^{24}$ a	$9(6) \cdot 10^{30}$ a
^{110}In $\rightarrow$ ^{110}Cd	EC	$1d_{5/2} - 0g_{9/2}$	$2.4(1) \cdot 10^{15}$ a	$3.0(2) \cdot 10^{14}$ a	$1.1(3) \cdot 10^{16}$ a
	β^+		$3.5(2) \cdot 10^{17}$ a	$3.8(3) \cdot 10^{16}$ a	$1.6(4) \cdot 10^{18}$ a
	EC/β^+		$2.30(8) \cdot 10^{15}$ a	$3.0(2) \cdot 10^{14}$ a	$1.1(3) \cdot 10^{16}$ a

Taulukko 10: Sama kuin taulukko 6 seitsemästi kielletyille siirtymille.

Siirtymä	Tyyppi	p–n-konf.	$t_{1/2}$(pnQRPA)	$t_{1/2}$(qp)	Arvioitu $t_{1/2}$
^{126}Sn $\rightarrow$ ^{126}Sb	β^-	$0g_{9/2} - 1f_{7/2}$	$1.9(2) \cdot 10^{20}$ a	$2.4(2) \cdot 10^{14}$ a	$9(2) \cdot 10^{20}$ a
^{132}Sn $\rightarrow$ ^{132}Sb	β^-	$0g_{9/2} - 1f_{7/2}$	$3.4(4) \cdot 10^{27}$ a	$7.4(6) \cdot 10^{14}$ a	$1.6(4) \cdot 10^{28}$ a